Friedrich-Alexander-Universität
Naturwissenschaftliche Fakultät

Bachelorarbeit

aus der Physik

Characterizing quasicrystals with topological quantities

Anna Milano

Betreuende Person: Prof. Dr. Michael Schmiedeberg

Abgabedatum: 14. April 2026

Abstract

In this work the dodecagonal Shield tiling is used as a model system to study flip induced tile rearrangements. A tile-based analysis is introduced in which the orientation of the tiles is encoded through complex phases that respect their rotational symmetry. This approach allows structural changes caused by flips to be quantified and their directional contributions to be analyzed.

The framework enables systematic investigations of flip processes and provides a basis for computational studies of larger regions. The approach can also be applied to other tilings in which flips occur.

Contents

1 Quasicrystals and Aperiodic Tilings

Soft condensed matter physics studies systems whose physical properties are strongly influenced by their internal structure. In many such systems, the macroscopic behavior emerges from the way simple entities arrange themselves to form complex structures on larger length scales. Understanding how local rules lead to global order is therefore a central question in this field. [1]

In solid state physics a crystal was traditionally defined as a structure that is both ordered and periodic. The atoms are arranged in a repeating unit cell that can be translated in space to generate the entire lattice. For a long time, it was believed that long range order necessarily implies translational periodicity. This view changed the world of physicists with the experimental discovery of quasicrystals by Dan Shechtman in 1984 in rapidly cooled Al-Mn alloys. [2] These materials exhibit sharp diffraction patterns that are characteristic for long range order but possess rotational symmetries that are forbidden in periodic crystals, such as fivefold or icosahedral symmetry. [3, 4] Their structure is therefore ordered, but not periodic. In fact, the theoretical framework of quasicrystals was already known to mathematicians before the physical discovery was made.

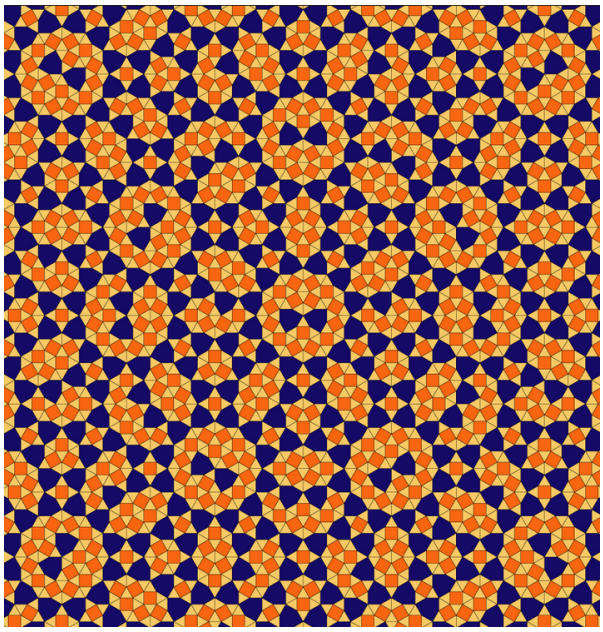

Figure 1: Local symmetry center of the Shield tiling [5]

The quasicrystalline order can often be described using mathematical tilings of the plane. In such tilings, a small set of prototiles fills the plane according to specific matching rules while forming an aperiodic structure. Although the resulting patterns lack translational periodicity, they still exhibit long range order and well defined symmetries. A well known example is the Penrose tiling, which demonstrates how aperiodic order can emerge

from simple geometric constrains. [4, 6] These tilings provide an important theoretical framework for studying quasicrystalline structures.

In addition to the usual phonon excitations known from periodic crystals, quasicrystals possess an additional type of mode called phasons. While phonons correspond to elastic displacements of atoms in the physical space, phasons describe rearrangements of the structure itself in the phase space. In the hydrodynamic description of quasicrystals, phonons and phasons form modes which do not change the free energy in the long wavelength limit. In tiling models these phasonic excitations often appear as local rearrangements of tiles. [7, 8]

In this context, the Shield tiling represents another interesting example of an aperiodic tiling. In the form shown in Figure 1 it was first described by Franz Gähler in [9]. The tiling consists of a set of prototiles that can cover the plane in a quasiperiodic way. As such, it provides a useful model system for studying structural rearrangements and relations between different tilings.

Such rearrangements in tilings can often occur through so called flips where a small cluster of tiles is transformed into an alternative configuration without changing the outer boundary. Studying these flips allows one to investigate how transformations influence the structure.

In the following sections, the Shield tiling will, therefore, serve as a model system to analyze rearrangements and the accessibility of different configurations within the tiling.

2 Detecting Structural Changes

To evaluate changes in a tiling, here in the form of phasonic flips, the orientation of each tile in the region of interest can be used. In order to do that, one first has to describe the tiles itself.
Shapes exhibiting j-fold symmetry have an orientation that is physically only defined up to modulo $2\pi/j$. The factor

$$\varphi_{\mathrm{j}} = \frac{2\pi}{j}$$

can therefore be introduced which takes the rotational symmetry of tiles into account. Once this is done, one can measure the orientation of the tile. For this, any vertex of the tile can be chosen and its corresponding angle can be read off using the unit circle. Combining φ_{j} with the measured angle θ one obtains

$$\Theta_{\mathrm{j}} = \theta \cdot \frac{1}{\varphi_{\mathrm{j}}}. \tag{2.1}$$

With this definition, the rotational invariance is automatically incorporated.
In order to evaluate the orientation, one can assign a complex number which consists of a complex phase

$$z_{\mathrm{n}} = a\ e^{2\pi i \Theta_{\mathrm{j}}}, \quad \mathrm{a} \in \mathbb{R} \tag{2.2}$$

to each tile with n being the number of the examined tile in a tile class. A tile class contains all tiles of the same kind. The coefficient a can be chosen arbitrarily. This definition corresponds to a complex orientational order parameter which is commonly used to describe rotational order in two dimensional systems. [7, 10, 11, 12]

As an example, consider one equilateral triangle in a tiling. The complex phase can be calculated by

$$\begin{aligned} z_1 &= e^{2\pi i \ \frac{\theta}{\frac{2\pi}{3}}} \\ &= e^{3i\theta}. \end{aligned} \tag{2.3}$$

An additional measurement of the angle for one vertex would result in an explicit expression for the phase. Having assigned said phase to each tile, one can sum over the phases of all tiles N in one tile class

$$Z = \sum_{\mathrm{n}=1}^{\mathrm{N}} z_{\mathrm{n}}, \quad \mathrm{N} \in \mathbb{N}. \tag{2.4}$$

The influence of the choice of a specific coordinate system, which is necessary to measure θ, can be removed by taking the square of the absolute value

$$q = |Z|^2. \tag{2.5}$$

This quantity defines a topological charge, which can then be evaluated further. Quantities of such a form are frequently used to characterize orientational order and topological defects in structures. [7, 11]

The formulas derived above can now be applied to a concrete example. As a suitable model system, the Shield tiling [9] is considered as mentioned above. It consists of three basic tiles which, when arranged appropriately, form an aperiodic structure. Specifically, the tiling consists of an equilateral triangle, a square and a six-sided shape which has the form of a shield as shown in Figure 2. Each of these tiles possesses a different rotational symmetry, which determines the form of the corresponding complex phase.

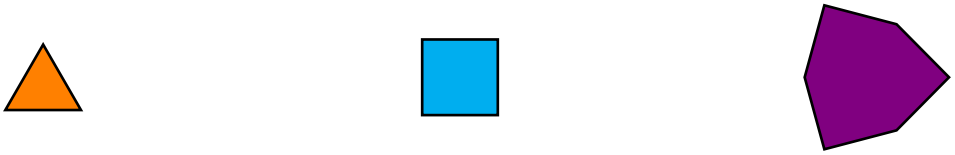

Figure 2: Prototiles of the Shield tiling [6]

For tiles with simple rotational symmetry, the phase follows directly from the symmetry. The equilateral triangle has threefold rotational symmetry, while the square has fourfold symmetry. Using Equation 2.2 the complex phase for these tiles can be written as

$$z_{\mathrm{T,n}} = e^{3i\theta} \tag{2.6}$$

$$z_{\mathrm{S,n}} = e^{4i\theta}. \tag{2.7}$$

For the shield tile however, finding a suitable expression is more subtle. The vertices alternate between the two interior angles $2\pi/3$ and $4\pi/3$. This alternating structure has to be taken into account in order to obtain a meaningful expression for the phase. Depending on the vertex at which the measurement is performed either, $2\pi/3$ or $4\pi/3$ has to be added. The vertices of the shield can be labeled by $k \in \mathbb{N}$. Due to mirror symmetry, the factor 2 appears in the exponent. The phase can be expressed by

$$z_{\mathrm{Sh,n}} = e^{2i(\theta+\phi)} \tag{2.8}$$

$$\phi = \begin{cases} \frac{2\pi}{3} & \text{for } 2k, \\ \frac{4\pi}{3} & \text{for } 2k+1. \end{cases}$$

3 Methods for Analyzing the Shield Tiling

In order to analyze transformations in the Shield tiling, one can introduce three complementary methods. These methods allow to describe rearrangements either in terms of individual tiles or in terms of the fundamental flip octagons.

3.1 Structure of Flips

When investigating possible flip types only a limited number of possibilities present themselves. The fundamental flip octagons in the Shield tiling are here, depicted by a purple shield, orange triangles, and a light blue square. After the flip, the octagons consist of a yellow shield, dark blue triangles, and a green square. A possible flip is shown in Figure 3.

Figure 3: Schematic flip which can occur in the Shield tiling. Left before a flip operation right after. Arrows indicate how the orientation of the flip octagon is measured [13]. Coloring of tiles serves only illustrative purposes.

In the tiling itself one observes twelve different possible orientations of flip octagons, as illustrated in Figure 4. Here, octagons which, lay opposite to each other form a flip pair, since the outer boundary is the same. The flip octagons can be identified by measuring the angle of the vertex where all tiles coincide in the direction of the acute angle of the shield which, opposes the square, as indicated in Figure 3 by the arrow. This line is also a symmetry axis.

To calculate the charge of each flip octagon one computes the complex phase of each tile in the octagon and, in contrast to above mentioned procedure where first one calculates the charge for each tile class separately, one sums all complex phases of any tile class and then computes the charge. If the phases were summed tile class by tile class, all flip octagons would yield the same charge $q = 4$ and the charge value could therefore not be used to distinguish between the different flip orientations.

The charge differences of flip partners in Table 1 are obtained by subtracting the charges of the flip octagons within each pair. For example, for the first pair $F_{12} \leftrightarrow F_6$ yields a charge difference of $\Delta q = q(F_6) - q(F_{12}) = 3 - (5 - 2\sqrt{3}) = -2 - 2\sqrt{3}$. Calculating Δq

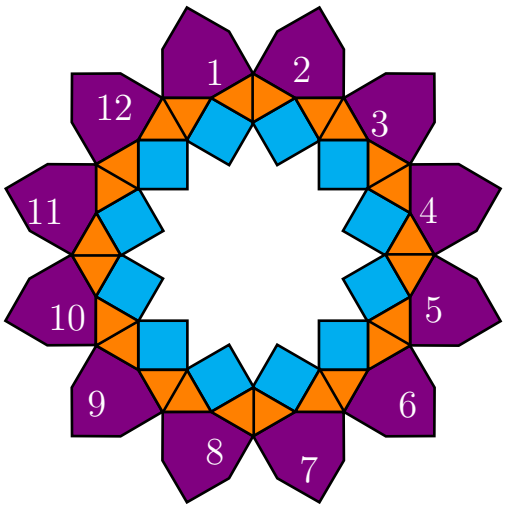

Figure 4: Possible flip partners in the Shield tiling

Flip F_i	θ	q	Flip partner	q_{flip}	$\Delta q = q_{\text{flip}} - q$
F_{12}	$\frac{9\pi}{12}$	$5-2\sqrt{3}$	F_6	3	$-2+2\sqrt{3}$
F_1	$\frac{7\pi}{12}$	2	F_7	6	4
F_2	$\frac{5\pi}{12}$	3	F_8	$5+2\sqrt{3}$	$2+2\sqrt{3}$
F_3	$\frac{3\pi}{12}$	3	F_9	$5+2\sqrt{3}$	$2+2\sqrt{3}$
F_4	$\frac{1\pi}{12}$	2	F_{10}	6	4
F_5	$\frac{23\pi}{12}$	$5-2\sqrt{3}$	F_{11}	3	$-2+2\sqrt{3}$
F_6	$\frac{21\pi}{12}$	3	F_{12}	$5-2\sqrt{3}$	$2-2\sqrt{3}$
F_7	$\frac{19\pi}{12}$	6	F_1	2	-4
F_8	$\frac{17\pi}{12}$	$5+2\sqrt{3}$	F_2	3	$-2-2\sqrt{3}$
F_9	$\frac{15\pi}{12}$	$5+2\sqrt{3}$	F_3	3	$-2-2\sqrt{3}$
F_{10}	$\frac{13\pi}{12}$	6	F_4	2	-4
F_{11}	$\frac{11\pi}{12}$	3	F_5	$5-2\sqrt{3}$	$2-2\sqrt{3}$

Table 1: Orientation angle θ, charge of the octagon q, flip partner, corresponding charge of the flip partner q_{flip} and charge differences Δq between the two charges

for each pair shows that the octagon pairs split up in different classes, namely

$$\begin{aligned}
\Delta q_{1+} &= \{(F_{12} \to F_6), (F_5 \to F_{11})\} = -2+2\sqrt{3},\\
\Delta q_{2+} &= \{(F_1 \to F_7), (F_4 \to F_{10})\} = 4,\\
\Delta q_{3+} &= \{(F_2 \to F_8), (F_3 \to F_9)\} = 2+2\sqrt{3},\\
\Delta q_{1-} &= \{(F_6 \to F_{12}), (F_{11} \to F_5)\} = 2-2\sqrt{3},\\
\Delta q_{2-} &= \{(F_7 \to F_1), (F_{10} \to F_4)\} = -4,\\
\Delta q_{3-} &= \{(F_8 \to F_2), (F_9 \to F_3)\} = -2-2\sqrt{3}.
\end{aligned} \tag{3.1}$$

The flip pairs that produce identical charge differences Δq are related by phases which are multiples of 30°. Pairs belonging to $\Delta q_{1\pm}$ can be mapped onto each other by a multiplication of $e^{\frac{\pi}{6}i}$, pairs which belong to $\Delta q_{2\pm}$ can be mapped by a multiplication of $e^{\frac{3\pi}{6}i}$ and pairs of $\Delta q_{3\pm}$ can be mapped by a multiplication of $e^{\frac{5\pi}{6}i}$.

As shown in Table 1 every charge can be written in the form

$$q(F_\mathrm{i}) = a + b\sqrt{3}, \quad a, b \in \mathbb{Z}. \tag{3.2}$$

Thus, all charges and charge differences lie in the ring

$$\mathbb{Z}\big[\sqrt{3}\big] = \{a + b\sqrt{3} | a, b \in \mathbb{Z}\}. \tag{3.3}$$

The set of all possible charge values build a ring which is generated by the phase factors

$$S = \left\{\frac{1}{2}(k + l\sqrt{3} + mi) \mid k, l, m \in \mathbb{Z}\right\}. \tag{3.4}$$

This ring is closed under 30° rotations and provides therefore, an algebraic structure for the possible flip charges. All complex phase contributions listed in Table 1 correspond to $\mathrm{Re}(S)$.

For convenience and to simplify the visualization of relations between different flip pairs, the charges will be represented in the following by vectors

$$\vec{q}_\mathrm{i} = \begin{pmatrix} a \\ b \end{pmatrix} \tag{3.5}$$

with respect to the basis vectors

$$\vec{b}_1 = \begin{pmatrix} 1 \\ 0 \end{pmatrix}, \ \vec{b}_2 = \begin{pmatrix} 0 \\ \sqrt{3} \end{pmatrix}. \tag{3.6}$$

This representation does not introduce an additional structure, but merely provides a compact way to keep track of the two coefficients.

Each flip pair listed in Table 1 can be assigned a vector $\vec{q}_\mathrm{i}$ corresponding to the charge difference Δq_i. Since every flip octagon has a unique partner located on the opposite side of Figure 4 the corresponding vectors occur in pairs with opposite sign meaning, for the first pair either $F_{12} \to F_6$ or $F_6 \to F_{12}$ can be identified which is also illustrated in Figure 5. This implies the relation

$$-\vec{q}_{i+} = \vec{q}_{i-}. \tag{3.7}$$

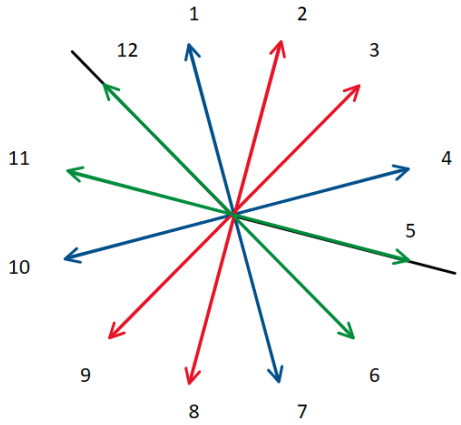

Figure 5: Sketch of the assignment of vectors corresponding to flip pairs. Green corresponds to $\Delta q_{1\pm}$, blue to $\Delta q_{2\pm}$ and red to $\Delta q_{3\pm}$. The black line divides the positive (12 - 5) and negative (6 - 11) direction of charge pairs.

Hence, one can define three charge difference vectors

$$\vec{q}_1 = \begin{pmatrix} -2 \\ 2 \end{pmatrix}, \quad \vec{q}_2 = \begin{pmatrix} 4 \\ 0 \end{pmatrix} \quad \text{and} \quad \vec{q}_3 = \begin{pmatrix} 2 \\ 2 \end{pmatrix}. \tag{3.8}$$

Evaluating Equation 3.8 reveals that the charge vectors are linearly dependent. For example, one can express $\vec{q}_3$ as

$$\vec{q}_3 = \vec{q}_1 + \vec{q}_2. \tag{3.9}$$

3.2 Flip-based Analysis

The different charges of the flips can now be used to characterize regions before and after an observed transformation. With the above introduced quantities one now can determine the flip octagons which are associated with the transformation. This can be done by comparing the charges of only the fundamental flips in the region, which is affected by the transformation.

First, one has to evaluate which region is affected by the transformation. This can be done by comparing both regions before and after the flip sequence and marking all tiles which changed their position. Then one identifies the flip octagons which are present in these areas. After that, one sums all the charges of said octagons in the changed region and all charges of the reference region before the transformation. The change can then be calculated by subtracting the sum of the reference region before the change from the

charge of the transformed region

$$\Gamma = \left(\sum_{\mathrm{i}=1}^{12} n_{\mathrm{i}}^{(\mathrm{flip})} \cdot q(F_{\mathrm{i}}) \right) - \left(\sum_{\mathrm{i}=1}^{12} n_{\mathrm{i}}^{(\mathrm{ref})} \cdot q(F_{\mathrm{i}}) \right), \quad n_{\mathrm{i}} \in \mathbb{N} \tag{3.10}$$

with $n_{\mathrm{i}}^{(\mathrm{flip})}$ being the multiplicity of the flip octagons in the region after a flip sequence and $n_{\mathrm{i}}^{(\mathrm{ref})}$ the multiplicity of the octagons in the unchanged region.

Since Γ again yields a charge value, one can use Equation 3.2 and write

$$\Gamma = A + B\sqrt{3} \quad A, B \in \mathbb{Z}$$

The charge difference Γ can be written as a vector and Equation 3.10 therefore corresponds to

$$\vec{\Gamma} = \begin{pmatrix} A \\ B \end{pmatrix} \tag{3.11}$$

expressed in the basis $\left(\vec{b_1}, \vec{b_2}\right)$ defined in Equation 3.6.

Solving these equations amounts in finding integer solutions for the multiplicities n_{i} that produce the observed coefficients A and B. The problem therefore reduces to solving a system of two linear equations.

Every observed transformation can thusly be associated with a vector whose entries (A, B) resemble coefficients and determine the possible combinations of the flips that can account for the observed change.

The vector $\vec{\Gamma}$ therefore characterizes the change induced by the flip octagons in the considered region and can also be used as a tool to create regions, which fulfill conditions one wants to impose.

3.3 Orientation-based Analysis

In order to analyze if after a flip sequence, an excess charge in one direction in terms of the flip pairs is detectable, one can write Equation 3.11 also in terms of the orientation

$$\vec{\Gamma} = u_1 \vec{q_1} + u_2 \vec{q_2} \tag{3.12}$$

where $\vec{q_{\mathrm{i}}}$ is the vector representation of Equation 3.1 and u_{i} is the multiplicity of the charge difference vector. Since $\vec{q_1}$ and $\vec{q_2}$ are linearly independent, the coefficients u_1 and u_2 are determined. The uniqueness will be discussed later in subsection 4.6.

In order to check whether a rearrangement of a region can be evaluated regarding the orientational change, one has to check if the two resulting equations of Equation 3.12

$$A = -2u_1 + 4u_2, \tag{3.13}$$
$$B = 2u_1 \tag{3.14}$$

are fulfilled. The orientation analysis can only be successfully applied if $\vec{\Gamma}$ corresponds to an integer combination of the charge difference vectors. If the observed change cannot be decomposed into such vectors, meaning the coefficients yield non integer solutions, the transformation contains isolated flip octagons and no directional excess can be defined.

3.4 Tile-based Analysis

One can also evaluate the net-change of a region before and after a transformation by subtracting the charges of all tiles in the reference region from the transformed region. The same can be done for the region, which actually changed by only calculating the tiles, which change before and after the flip sequence.

$$\Delta q_{\text{tot}} = q_{\text{tot,flip}} - q_{\text{tot,ref}} \tag{3.15}$$
$$\Delta q_{\text{ch}} = q_{\text{ch,flip}} - q_{\text{ch,ref}} \tag{3.16}$$

The quantities Δq_{tot} and Δq_{ch} can also be interpreted as measurable charge differences of the transformation. For a given charge change Δq, the coefficients A and B of the corresponding charge vector can be determined. In a first step, these entries allow one to generate the number of flips contributing to the transformation. However, since the tile charges originate from different tile classes, the (re-)construction of the flip sequence is in general not unique.
In contrast to the flip based description, the tile based analysis involves several tile classes which additionally inhibit different possible charge values. Consequently, the same total charge difference may correspond to different rearrangements of the tiles.

4 Charge Analysis of Flip Transformations

In the following examples the flip processes are illustrated by explicit flip sequences. These sequences represent one possible way to realize the corresponding charge difference. In general, however, the charge vector $\vec{\Gamma}$ alone does not uniquely determine the flip sequence. This will also be discussed in subsection 4.6.

4.1 Single Flip Transformation

As a first example, one can consider a small patch consisting of four shields, four triangles and a central square. The purpose of this example is to demonstrate how flip-based analysis introduced in the previous section can be used to characterize a local transformation which cannot be fully done by the tile-charges alone. Finally, the orientation analysis reveals the directional character of the transformation.

An octagonal region is selected for a change and is shown in Figure 6. The resulting orientations as complex phases of the tiles before and after the transformation are listed in Table 2 and Table 3.

Figure 6: Reference region (left) and the same region with an incorporated single flip (right). The flipped tiles are colored according to the choice made in section 2

Triangle	θ	z	Square	θ	z	Shield	θ	z
1	0	1	1	$\frac{19\pi}{12}$	$\frac{1}{2}+\frac{\sqrt{3}}{2}i$	1	$\frac{7\pi}{12}+\frac{4\pi}{3}$	$\frac{\sqrt{3}}{2}-\frac{i}{2}$
2	$\frac{6\pi}{12}$	$-i$				2	$\frac{13\pi}{12}+\frac{4\pi}{3}$	$\frac{-\sqrt{3}}{2}+\frac{i}{2}$
3	$\frac{12\pi}{12}$	-1				3	$\frac{19\pi}{12}+\frac{4\pi}{3}$	$\frac{\sqrt{3}}{2}-\frac{i}{2}$
4	$\frac{18\pi}{12}$	i				4	$\frac{1\pi}{12}+\frac{4\pi}{3}$	$\frac{-\sqrt{3}}{2}+\frac{i}{2}$

Table 2: Angle and resulting complex phase of all tiles in the reference region before the transformation. Triangles and shields numbered counterclockwise starting at the tiles on top

Triangle	θ	z	Square	θ	z	Shield	θ	z
1	0	-1	1	$\frac{19\pi}{12}$	$\frac{1}{2}+\frac{\sqrt{3}}{2}i$	1	$\frac{7\pi}{12}+\frac{4\pi}{3}$	$\frac{\sqrt{3}}{2}-\frac{i}{2}$
2	0	-1				2	$\frac{1\pi}{12}+\frac{4\pi}{3}$	$\frac{-\sqrt{3}}{2}+\frac{i}{2}$
3	$\frac{18\pi}{12}$	i				3	$\frac{19\pi}{12}+\frac{4\pi}{3}$	$\frac{\sqrt{3}}{2}-\frac{i}{2}$
4	$\frac{18\pi}{12}$	i				4	$\frac{1\pi}{12}+\frac{4\pi}{3}$	$\frac{-\sqrt{3}}{2}+\frac{i}{2}$

Table 3: Angle and resulting complex phase of all tiles in the patch after the transformation. Triangles numbered from top right to left and bottom left to right and shields from top to bottom

charge	ref. region	ref. region + flip	change ref. region	ch. ref. region + flip
q_{T}	0	8	2	2
q_{S}	1	1	1	1
q_{Sh}	0	0	1	1

Table 4: Charge of the whole reference region where every tile is included, the same region after flips were performed, only the charge of tiles which are affected by the change and the affected region after the change

As a first step, the transformation is analyzed using the tile-based charges introduced in subsection 3.4.

Comparing the charges of both regions in Table 4 one finds that only the charge of the squares q_{S} remains unchanged before and after the flip in both the whole region and the changed region. In contrast, the charge of the triangles q_{T} increases when the entire reference region is considered, while it stays constant within the changed region. The charge of the shields q_{Sh} behaves oppositely. It increases in the changed region but remains zero when the full reference region is taken into account.

Adding all resulting charges of the selected region before and after the flip results in

$$q_{\mathrm{tot,flip}} - q_{\mathrm{tot,ref}} = (8+1) - 1 = 8 = \Delta q_{\mathrm{tot}}.$$

Considering only the region in which the tiles change before and after the flip yields

$$q_{\mathrm{ch,flip}} - q_{\mathrm{ch,ref}} = 4 - 4 = 0 = \Delta q_{\mathrm{ch}}.$$

This result would suggest that no change occurred in the affected region since the summed tile charge in the region of change yields no change. However, the local arrangement of tiles is clearly different after the transformation. This demonstrates, that the tile-based charge alone is not sufficient to characterize the transformation.

To resolve this ambiguity, one can apply the flip-based analysis introduced in subsection 3.2 and identify the corresponding flip octagons.

Following Equation 3.10 the change induced by the transformation can be expressed as a linear combination of the charges of the flip octagons. In the present example, the region before the transformation contains flip octagon F_{10} while after the change, the region inherits F_4. The change is therefore given by

$$\Gamma = q(F_4) - q(F_{10}) = 2 - 6 = -4$$

Which results in

$$\vec{\Gamma} = \begin{pmatrix} -4 \\ 0 \end{pmatrix}.$$

To interpret this transformation within the orientational framework, the vector $\vec{\Gamma}$ can be decomposed into the directions introduced in Equation 3.1. From these values, the orientation and excess follow directly

$$\vec{\Gamma} = -\vec{q}_2.$$

This example illustrates the difference of the two analysis methods. While the tile-based charge suggests that no change occurred in the affected region, the flip-based analysis correctly identifies the transformation as an exchange of the flip octagons F_{10} and F_4.

The orientational analysis shows that the transformation corresponds to a single step in the $-q_2$ direction.

Hence, the observed transformation can be interpreted as a specific linear combination of the flip charges, demonstrating how local tiling transformations can be represented within the vector space introduced in subsection 3.2.

4.2 Compensating Flip Pairs

The flip-based description can also be applied to transformations that involve several neighboring flips. In such cases, several flip pairs may appear simultaneously, and their contributions to the total flip charge can cancel. This example shows, how the flip-based analysis identifies these processes.

charge	ref region	ref. region + flip	change ref. region	ch ref. region + flip
q_{T}	0	16	4	4
q_{S}	0	0	0	0
q_{Sh}	12	12	12	3

Table 5: Charge of the whole reference region where every tile is included, the same region after flips were performed, only the charge of tiles in the region which is affected by the transformation and the same region after the change

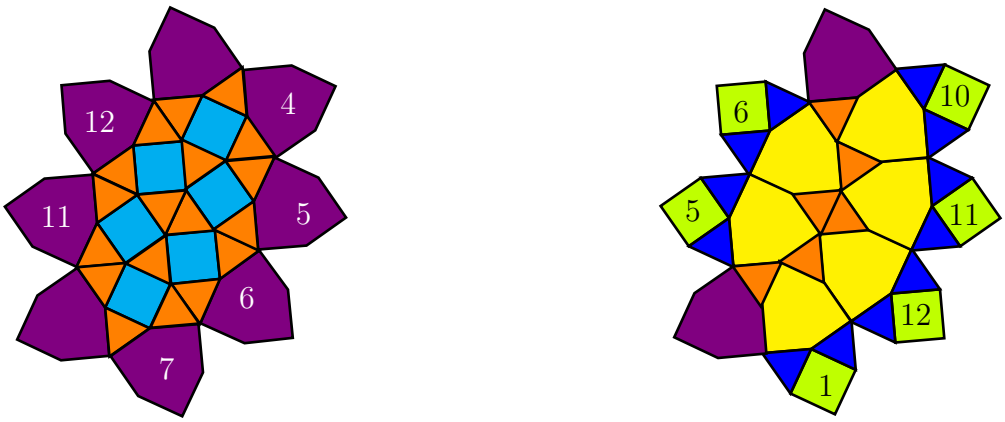

Figure 7: Reference region (left) and transformed region (right) in which, flip pairs appear. Identifiable flip octagons are marked with their corresponding number

Comparing the charges before and after the transformation in Table 5 shows that only the square charges q_S do not change, while the charge of the triangles and shields are affected. When the analysis is restricted to the changed region, the behavior of the charges differs. The triangle charge remains constant, while the shield charge decreases. In contrast, when the full reference region is considered, the shield charge remains unchanged and the triangle charge increases.

To obtain a clearer description of this transformation, the region can instead be analyzed in terms of the flip-based framework. For this, the regions can be decomposed into the contained flip octagons

$$q_{\text{tot,flip}} - q_{\text{tot,ref}} = (16 + 12) - 12 = 16 = \Delta q_{\text{tot}}.$$

Restricting the evaluation to the region in which the tiles actually change yields

$$q_{\text{ch,flip}} - q_{\text{ch,ref}} = 7 - 16 = -9 = \Delta q_{\text{ch}}.$$

Evaluating only the region in which a change occurs, the flip octagons of the pairs $F_{11} \leftrightarrow F_5$ and $F_{12} \leftrightarrow F_6$ only change their positions and remain present in the region before and after the transformation. The transformations, $F_7 \rightarrow F_1$ and $F_4 \rightarrow F_{10}$ are the only ones for which both members of the corresponding flip pair are not simultaneously

present in the region which shows in the calculation of

$$\begin{aligned}\Gamma &= \Big(q(F_5) + q(F_6) + q(F_{10}) + q(F_{11}) + q(F_{12}) + q(F_1)\Big) \\ &- \Big(q(F_{11}) + q(F_{12}) + q(F_4) + q(F_5) + q(F_6) + q(F_7)\Big) \\ &= \Big((5 - 2\sqrt{3}) + 3 + 6 + 3 + (5 - 2\sqrt{3}) + 2\Big) \\ &- \Big(3 + (5 - 2\sqrt{3}) + 2 + (5 - 2\sqrt{3}) + 3 + 6\Big) \\ &= 0.\end{aligned}$$

The resulting flip charge is therefore

$$\vec{\Gamma} = \begin{pmatrix} 0 \\ 0 \end{pmatrix}.$$

The vanishing flip charge can be understood more clearly within the orientation-analysis which resolves the directional contributions of the individual flips. The total charge difference can be written as

$$\vec{\Gamma} = 2\vec{q_1} - 2\vec{q_1} + \vec{q_2} - \vec{q_2} = \vec{0}.$$

The transformation consists of two flips in opposite directions whose contributions cancel exactly. The vanishing flip charge therefore does not imply that no transformation occurred. Instead, it indicates that the initial and final arrangements belong to the same flip change class. Therefore transformations with $\vec{\Gamma} = 0$ corresponds to rearrangements of the flips within the same equivalence class defined in Equation 3.1, which preserve the total flip charge while still producing local charges in the tiling.

4.3 Loss of Identifiable Flip Octagons

After introducing the possibility of rotations of the dodecagons in discrete steps of 30° in subsection 8.1 it becomes, easier to analyze and arrange changes in the tiling. In the following examples, flip octagons located inside a dodecagon whose squares share a vertex are preferred identified. For example F_8 and F_7 in Figure 8 fulfill this property.

In larger rearrangements of the tiling it may occur that the number of identifiable flip octagons within a considered region changes during the transformation. Some flip octagons may move into or out of the region, while others may disappear in the defined form because the surrounding tiles change. In such cases the initial tiles are still present, but their relative positions no longer form the characteristic from, required to identify a flip octagon.
For example, the square belonging to a flip octagon may shift to a different position and

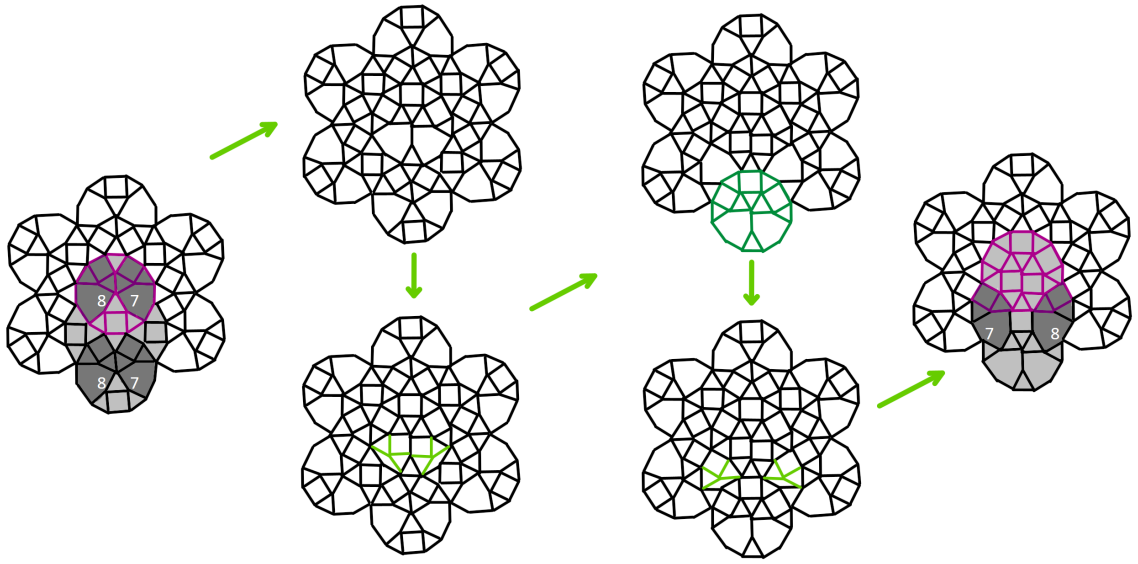

Figure 8: Sequence of flips within in a larger region in which the total charge is conserved. Light gray indicates regions which alter before and after the change. Dark gray areas indicate identified flip octagons. Sketched flips are shown in light green and rotated dodecagons are drawn in dark green. Pink regions mark the center of the patch.

can thusly no longer be identified as it is the case in the transformation in Figure 8. Importantly, this change is not caused by boundary effects. Even when a larger region is considered as shown in Figure 9, to additional flip octagons appear. This indicates that the observed effect is not due to missing contributions outside the region, but results from the local rearrangement itself.

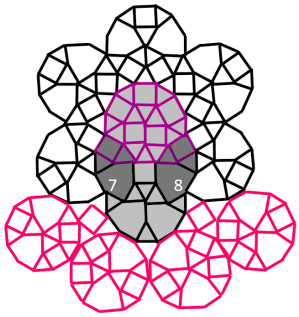

Figure 9: Enlarged region of Figure 8 sketched in pink which is not affected by the flip sequence. Shields in the black bottom dodecagon can also not be identified as part of flip octagons considering tiles outside the examined region. This rules boundary effects out

To analyze how such changes affect the balance, the corresponding charge differences are evaluated again for both the entire region and the changed region.

The total charge of the considered region

$$q_{\text{tot,flip}} - q_{\text{tot,ref}} = 49 - 49 = 0 = \Delta q_{\text{tot}}$$

remains unchanged, which shows that the transformation conserves the charge of the configuration.

Considering only the region in which the tiles change before and after the flip yields

$$q_{\text{ch,flip}} - q_{\text{ch,ref}} = 17 - 17 = 0 = \Delta q_{\text{ch}}.$$

Thus, also within the light gray area, the total charge remains conserved. However, the conservation of the tile charge does not necessarily imply that the flip structure of the region remains unchanged.

To analyze this in more detail, the transformation can be decomposed into the corresponding flip octagons. The calculation of the change of flip octagons yields

$$\begin{aligned}\Gamma &= \big(q(F_7) + q(F_8)\big) - \big(2 \cdot q(F_7) + 2 \cdot q(F_8)\big) \\ &= \big(11 + 2\sqrt{3}\big) - \big(22 + 4\sqrt{3}\big) = -11 - 2\sqrt{3}\end{aligned}$$

and can be written as

$$\vec{\Gamma} = \begin{pmatrix} -11 \\ -2 \end{pmatrix}$$

To perform the orientation analysis, the charge vector $\vec{\Gamma}$ would have to be expressible as an integer linear combination of the directions defined in subsection 3.2. Writing

$$\begin{gathered}\vec{\Gamma} = u_1 \cdot \vec{q_1} + u_2 \cdot \vec{q_2} \\ \begin{pmatrix} -11 \\ -2 \end{pmatrix} = u_1 \begin{pmatrix} -2 \\ 2 \end{pmatrix} + u_2 \begin{pmatrix} 4 \\ 0 \end{pmatrix}\end{gathered}$$

yields

$$u_1 = -1 \quad \text{and} \quad u_2 = -\frac{13}{4}$$

Since the coefficients are not integers, the charge difference cannot be written as a combination of the flip directions, and an excess charge in one direction cannot be detected. Consequently, the resulting value of Γ indicates that the transformation cannot be decomposed into flip pairs.

While the tile-based analysis shows that the total tile charge is conserved, the flip based description reveals that the transformation cannot be fully expressed within the defined flip directions. This demonstrates that the flip charge provides additional information about the structure of the tiling which is not captured by the tile charges alone but also shows that this alone is not sufficient to describe all rearrangements in the tiling.

This mismatch therefore reflects a limitation of the flip bases representation and not a boundary effect or an insufficiently large region.

4.4 Unpaired Flip Octagons

In larger rearrangements, it may occur that the flip octagons present in a region cannot be paired locally. Some flip octagons remain unpaired within the considered region either in the reference region or after the transition. In such situations a change may arise even through the tile charge of the region being conserved.

Before hand, in previous examples the flip octagons were identified by selecting those in which the two squares of two flips shared a vertex. If such a choice is not possible, another flip within the same dodecagon can be selected for identification. The octagons F_4 and F_{11}, labeled yellow, in Figure 10 demonstrate this.

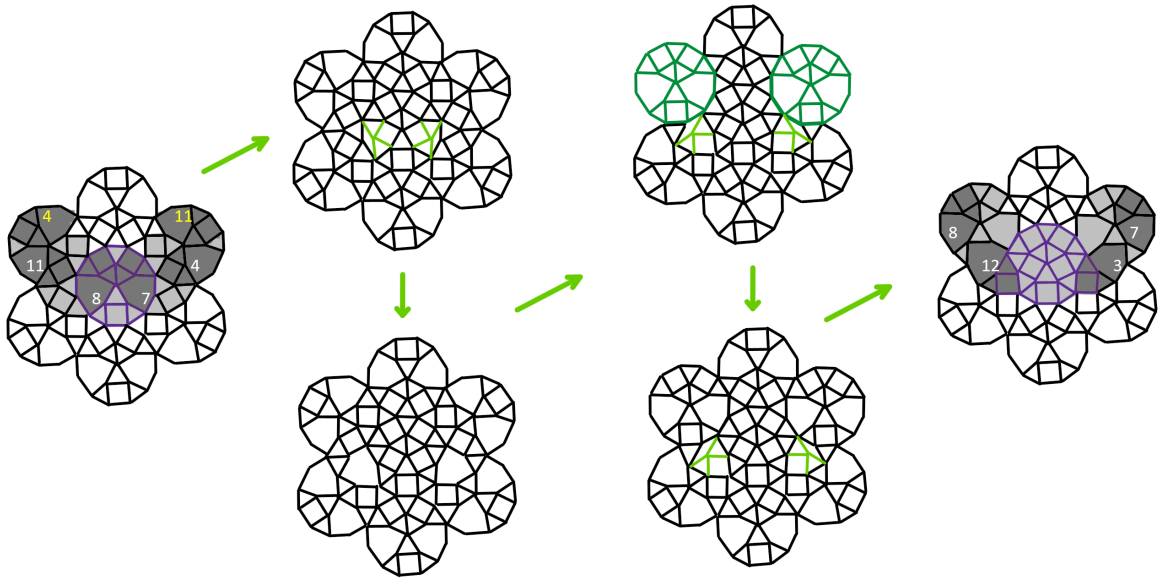

Figure 10: Sequence of flips within in a larger region in which the total charge is conserved. Light gray indicates regions which alter before and after the change. Dark gray areas indicate identified flip octagons. Sketched flips are shown in light green and rotated dodecagons are drawn in dark green. Purple regions mark the center of the patch. Yellow labels mark a different identification of the flip octagons

The total charge of the considered region

$$q_{\text{tot,flip}} - q_{\text{tot,ref}} = 49 - 49 = 0 = \Delta q_{\text{tot}}.$$

remains unchanged, which shows that the entire region preserves the total tile charge.

However, restricting the evaluation to the region in which the tiles actually change yields

$$q_{\text{ch,flip}} - q_{\text{ch,ref}} = 21 - 26 = 5 = \Delta q_{\text{ch}}.$$

This indicates that even though the total tile charge remains conserved, the charges are redistributed within the locally changing region.

To analyze how this redistribution is related to the underlying flip structure, the transformation can be decomposed to the corresponding flip octagons. The flip octagons F_7 and F_8 are not included in the charge calculation because they appear both before and after the transformation and only change their position within the region. They therefore correspond to a translation of the existing flip octagons and do not contribute to the flip change

$$\Gamma = \Big(q(F_{12}) + q(F_3)\Big) - \Big(2 \cdot q(F_{11}) + 2 \cdot q(F_4)\Big) = \big(8 - 2\sqrt{3}\big) - 10 = -2 - 2\sqrt{3}.$$

$$\vec{\Gamma} = \begin{pmatrix} -2 \\ -2 \end{pmatrix}$$

In terms of the excess charge, one can calculate

$$\begin{pmatrix} -2 \\ -2 \end{pmatrix} = u_1 \begin{pmatrix} -2 \\ 2 \end{pmatrix} + u_2 \begin{pmatrix} 4 \\ 0 \end{pmatrix}$$

which yields

$$u_1 = -1 \quad \text{and} \quad u_2 = -1.$$

Therefore,

$$\vec{\Gamma} = -\vec{q}_1$$

which corresponds to a negative excess charge.

The value of Γ indicates that the movement of the flip octagons correspond, to a combination of flips which is not trivial even through the global charge remains conserved.

This example therefore illustrates that even if the global charge of a region is conserved, the presence of unpaired flip octagons can lead to a non vanishing charge. The flip-based description therefore captures structural information about the rearrangement of the tiling that is not directly visible in the tile charge analysis.

4.5 Additional Cases of Unpaired Flip Octagons

The previous example showed that unpaired flip octagons can lead to a non zero flip charge. The transformation shown in Figure 11 provides a further example in which several flip octagons remain unpaired within the considered region.

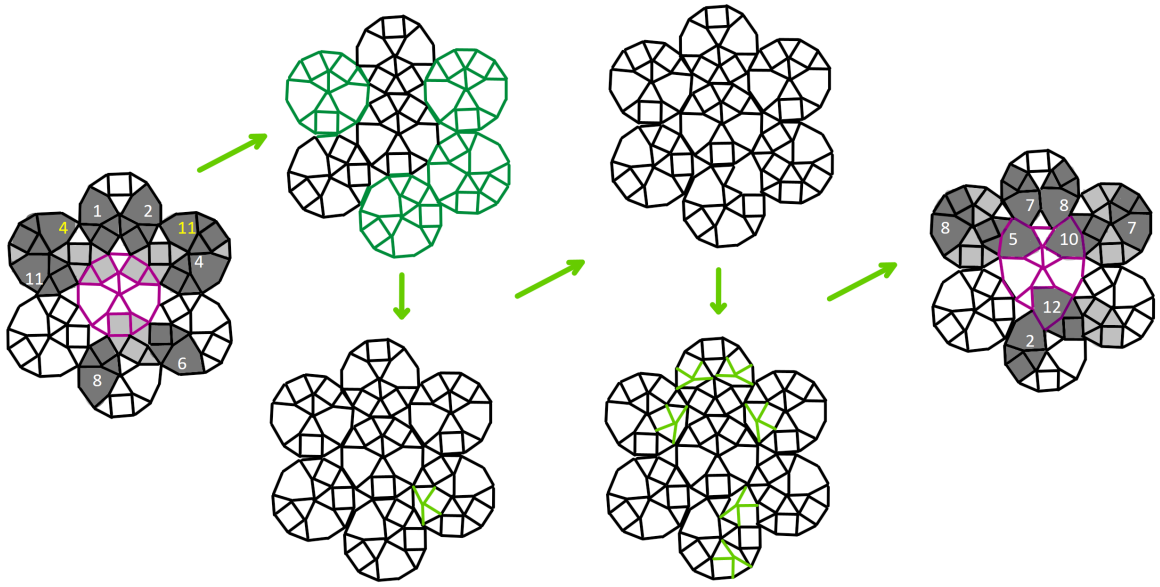

Figure 11: Sequence of flips within in a larger region in which the total charge is conserved. Light gray indicates regions which alter before and after the change. Dark gray areas indicate identified flip octagons. Sketched flips are shown in light green and rotated dodecagons are drawn in dark green. Pink regions mark the center of the patch. Yellow labels mark a different identification of the flip octagons

Again, the total charge of the considered region,

$$q_{\text{tot,flip}} - q_{\text{tot,ref}} = 49 - 49 = 0 = \Delta q_{\text{tot}}.$$

remains conserved.

Restricting the region in which the tiles actually change yields

$$q_{\text{ch,flip}} - q_{\text{ch,ref}} = 21 - 9 = 12 = \Delta q_{\text{ch}}.$$

To understand the origin of this change, the transformation can be decomposed again into the corresponding flip octagons. A comparison of the region before and after the transformation shows that several flip octagons can be paired, namely $F_{11} \to F_5$, $F_4 \to F_{10}$, $F_1 \to F_7$, $F_2 \to F_8$, $F_6 \to F_{12}$ and $F_8 \to F_2$ leaving F_{11}, F_4 before and F_8 and F_7 unpaired after the transformation. It is observed that the unpaired flip octagons occur twice in the associated regions.

Calculating the charge differences of the flips while leaving out $F_2 \leftrightarrow F_8$ because they

cancel each other out yields

$$\begin{aligned}\Gamma &= \big(q(F_5) + q(F_{10}) + q(F_7) + q(F_{12}) + q(F_8) + q(F_7)\big) \\ &\quad - \big(q(F_{11}) + q(F_4) + q(F_1) + q(F_6) + q(F_{11}) + q(F_4)\big) \\ &= 15 - \big(33 - 2\sqrt{3}\big) = -18 + 2\sqrt{3}.\end{aligned}$$

This corresponds to the charge vector

$$\vec{\Gamma} = \begin{pmatrix} -18 \\ 2 \end{pmatrix}$$

Calculating the multiplicities of the charge difference vectors by inserting $\vec{\Gamma}$ in Equation 3.12 and solving the equation yields

$$u_1 = 1 \quad \text{and} \quad u_2 = -4.$$

Therefore,

$$\vec{\Gamma} = \vec{q_1} - 4\vec{q_2}$$

which corresponds to a negative excess charge.

The resulting value of Γ reflects the presence of several unpaired flip octagons within the considered region. While a number of flip octagons can be matched between the reference and transformed region, this example demonstrates that multiple unpaired flip octagons can accumulate and produce a larger flip charge.

4.6 (Re-)construction of Flip Sequences

After the evaluation in previous examples in which a minimal sequence of flips was evaluated through the orientational analysis, one can ask whether it is also possible to (re-)construct a flip sequence solely from a given value of the change $\vec{\Gamma}$.

When only the initial and final regions in Figure 12 are compared, the resulting charge difference is

$$\begin{aligned}\Gamma &= q(F_5) - q(F_{11}) = 2 - 2\sqrt{3} = \Delta q_{1-} \\ \vec{\Gamma} &= \begin{pmatrix} 2 \\ -2 \end{pmatrix} = -\vec{q_1}\end{aligned}$$

which represents the net change of the region. However, when summing the contributions of the explicitly constructed flip sequence, which is shown in Figure 12 on top, a larger

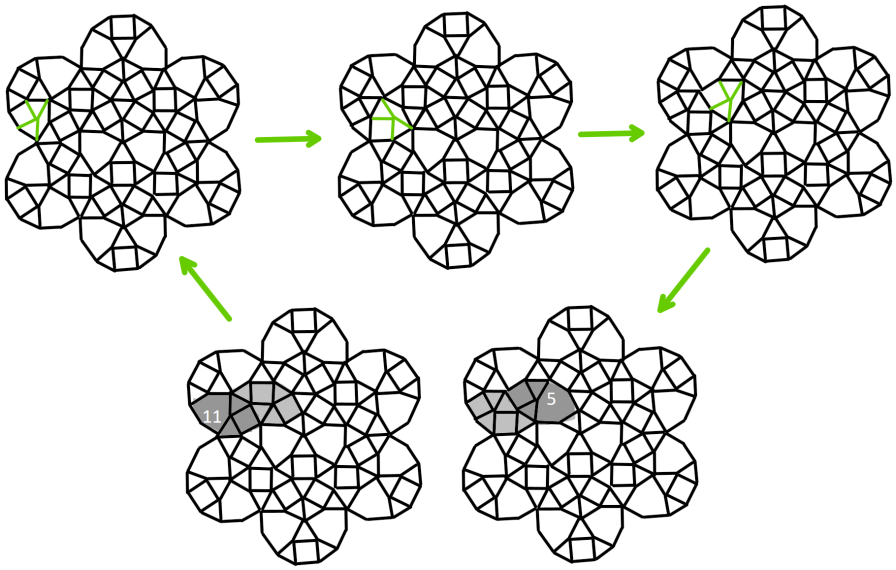

Figure 12: Construction of a flip sequence. The top row shows an explicitly constructed sequence of flips connecting two regions, while the comparison of the initial and final region on the bottom yields the charge difference $\vec{\Gamma}$

value,

$$\vec{s} = \begin{pmatrix} 2 \\ -6 \end{pmatrix} = -\vec{q}_1 + \vec{q}_3 - \vec{q}_1$$

is obtained.

The start-end comparison therefore measures a minimal charge change, while the full flip sequence reflects the actual path taken through intermediate configurations. Moreover, the charge difference $\vec{\Gamma}$ does not uniquely determine the flip process even on the level of individual flips because, every obtained directional contribution allows two different possible flips as shown in Equation 3.1. The result of $\vec{\Gamma}$ corresponds to a single flip, which would correspond to the first step in the flip sequence shown top left in Figure 12. But the same net change can also be obtained from larger sequences of flips. The explicitly constructed sequence shown in Figure 12 provides such an example. Although the total contribution of the constructed flip sequence $\vec{s}$ differs from the minimal flip sequence obtained $\vec{\Gamma}$, the same final change charge is obtained.
This shows that different flip sequences can lead to the same charge difference $\vec{\Gamma}$. Consequently, when only the value of $\vec{\Gamma}$ is known, a flip sequence can be constructed, but in this framework not uniquely.

Concluding, the presented examples demonstrate how different arrangements of flip octagons affect the quantities Δq_{tot}, Δq_{ch} and the flip charge Γ.
In the first examples, the total tile charge is not conserved. The observed charges can be explained by the presence of individual flips of balanced flip pairs, which either introduce

a contribution or cancel each other, resulting in a vanishing contribution.
In subsequent examples, the total tile charge remains conserved, indicating that the transformations correspond mainly to rearrangements within the considered region. These rearrangements become observable through changes in Δq_{ch} and Γ, which reveal the effects of the distribution of tiles and the movements of flip octagons in the region.
In addition, the vectorial quantity $\vec{\Gamma}$ provides additional information about the change in the system because it encodes the directional contribution of the flips within the region. The (re-)construction example further illustrates a limitation of this description. Although the charge difference $\vec{\Gamma}$ characterizes the flip change between two configurations, it does not uniquely determine the resulting region. Different flip sequences can produce the same value of $\vec{\Gamma}$, leading to different intermediate configurations and final regions.

5 Generating Different Tilings by Flips

An interesting observation made in [14] is the influence of Barium on Titanium-Oxide rings that causes an alternation in the structure. After the probe is equipped with a tessellation, the change can be broken down to a transformation from one tiling to another. Hence, the question how different tilings can be obtained by only using flips will be investigated now.

5.1 Shield Triangle Tiling

In order to study this first, a single dodecagon is considered as the smallest possible reference region. As a first step, an investigation of possible transformations within such a structure is examined.

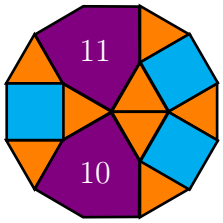

Figure 13: Arbitrary dodecagon found frequent inside the Shield tiling

One can now modify the region in a fundamentally different way compared to the previous examples. A possible rearrangement inside the dodecagon contains four triangles and two additional shields, which fill the space. The crucial feature of this changed region is that all squares are removed from the region.

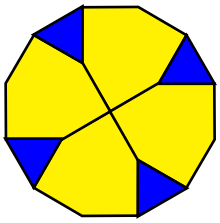

Figure 14: Dodecagon consisting of only shields and triangles

First, comparing the tile-charges before and after the flip, the triangle charge q_{T} and the shield charges q_{Sh} change, while the square charge q_{S} remains unchanged as summarized in Table 6.

$$q_{\mathrm{tot,flip}} - q_{\mathrm{tot,ref}} = 0 - (4+3) = -7 = \Delta q_{\mathrm{tot}}.$$

charge	ref region	ref region + flip	change ref. region	ch ref. region + flip
q_{T}	4	0	2	2
q_{S}	0	0	0	0
q_{Sh}	3	0	3	0

Table 6: Charge of the reference region without a flip and the same region with and an embedded flip

$$q_{\mathrm{ch,flip}} - q_{\mathrm{ch,ref}} = 2 - 5 = -3 = \Delta q_{\mathrm{ch}} \tag{5.1}$$

Evaluating the flip charge difference yields

$$\Gamma = 0 - (q(F_{10} + q(F_{11})) = -9$$
$$\vec{\Gamma} = \begin{pmatrix} -9 \\ 0 \end{pmatrix}.$$

For the orientational analysis, one gets

$$\vec{\Gamma} = u_1 \cdot \vec{q}_1 + u_2 \cdot \vec{q}_2$$
$$\begin{pmatrix} -9 \\ 0 \end{pmatrix} = u_1 \begin{pmatrix} -2 \\ 2 \end{pmatrix} + u_2 \begin{pmatrix} 4 \\ 0 \end{pmatrix}$$

yields

$$u_1 = 0 \quad \text{and} \quad u_2 = -\frac{9}{4}$$

Since this result suggests that the change cannot be expressed through the flip pairs, it raises the question whether such a transformation can despite this be described as a sequence of elementary flips. In particular, considering the region shown in Figure 14 one can ask if it is possible to construct a sequence of flips that produces a region consisting solely of such dodecagons without any squares. Such a configuration would consequently lead to a different tiling.

So, the question arises whether it is possible to construct another tiling from an initial one by solely performing a sequence of elementary flips? In other words, are these two tilings *connected*/flip accessible to each other? [15]

5.1.1 Flip Grid

To investigate first if the whole plane can be covered with such dodecagons which do not consist of squares, possible arrangements that could generate such regions are analyzed. In particular, the possibility of the construction of the Shield-Triangle tiling proposed in [16] by starting from arrangements in the Shield tiling is investigated. The tiling uses

the same prototiles as the Shield tiling without the squares. If it were possible to reach this structure through flips, the squares present in the original tiling would effectively disappear. Two constructions of such tilings are discussed in [16]. In the following, they are briefly reviewed and analyzed whether they can arise from sequences of flips

The first is the Shield-line tiling. As the name already suggests, the construction is based on lines, which consist of a shield and adjacent triangles, as shown in Figure 15.

Figure 15: Sketched Shield-line tiling with uniform orientation composed of flip octagons based on the work in [16]

This mechanism is a promising candidate to eliminate the squares because one could always flip along one line. But considering any region (e.g. Figure 20) of the perfect tiling, one notices that it is not possible to perform a flip to get two flip octagons aligned in the right way, as depicted in Figure 15 in such a way that the surrounding tiles are also in the right position for a following flip. So, a Shield-Line tiling cannot be derived from the Shield tiling.

Since the Shield-line construction cannot be generated through flips starting from the Shield tiling one can turn to the second construction shown in Figure 16 proposed in [16].

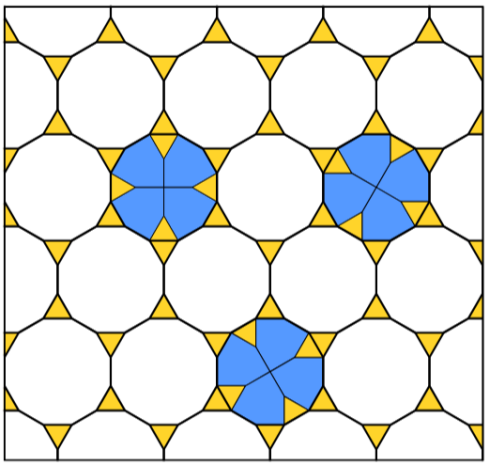

Figure 16: Sketch of how to construct the Shield triangle tiling with three different ways of how the interior of the dodecagons have to be arranged [16]

To study whether such a structure could arise through flips, a minimal arrangement which produces aligned shields after a flip is shown in Figure 17. These configurations will be called *super-tiles* from now on.

(a) super-tile before the flip

(b) super-tile after flip

Figure 17: Super-tiles before and after a possible flip which can be used to construct a Shield-Triangle Tiling

Now, considering Figure 16 yields only three different orientations for the arrangement of the super-tiles. They are shown in Figure 18.

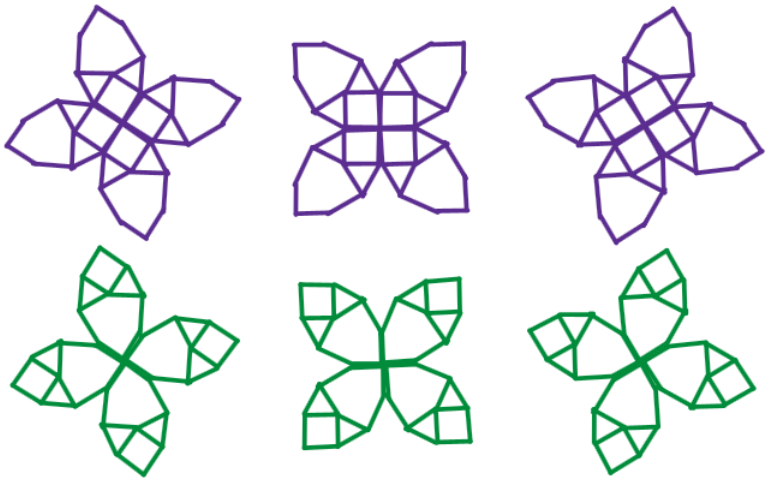

Figure 18: Sketch of possible orientations for the building blocks. In purple before, in green after the flip

The key idea is now to investigate whether these super-tiles can tessellate the plane in such a way that all squares eventually disappear through flips. In order to do this one can construct a large region consisting of these super-tiles arranged in a grid like structure. If the super-tiles are arranged as shown in Figure 19a one obtains a large region of connected shields. However, this arrangement does not yet form a valid tiling since gaps remain between neighboring super-tiles. The space can only be filled with one square in the middle and four adjacent triangles, as shown in Figure 19b. After performing the flips shown in Figure 19c all possible flip configurations are exhausted. The remaining squares are embedded in environments where the edge orientations of the

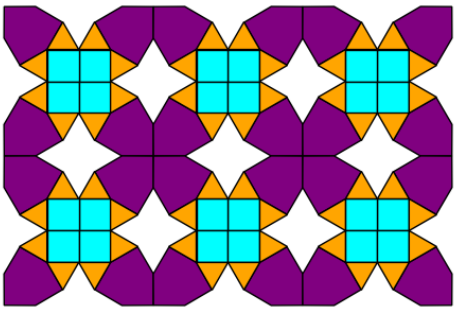

(a) Grid build from an ideal starting position of all building blocks

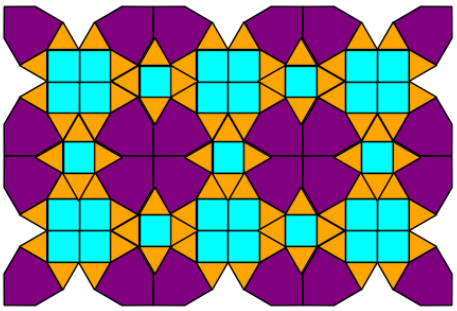

(b) Filling empty spaces in the grid with the only possible option: one square and four triangles

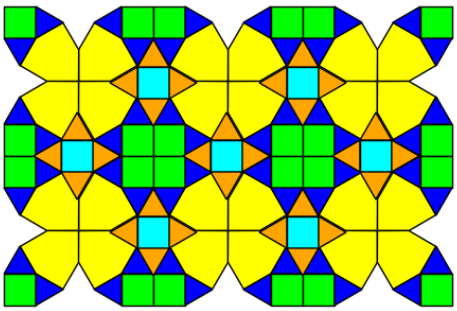

(c) Grid after flipping all octagons from which the grid was originally build

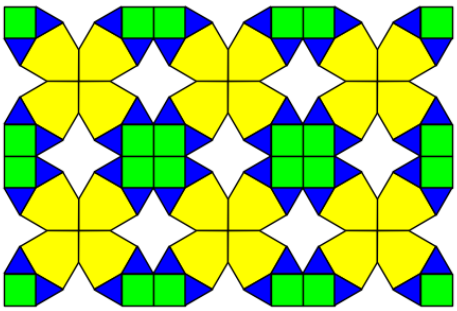

(d) The same grid without filled spaces

Figure 19: Performing flips in the ideal grid for the Shield-Triangle tiling

surrounding tiles prevent the formation of new flips, since one obtains after the flips the starting arrangement which is just shifted. This is easy to see if one compares Figure 19a and Figure 19d. Therefore, even though the super-tile construction allows the creation of extended regions of connected shields, the mechanism inevitably produces squares that cannot be obtained from the prototiles of the Shield tiling through a sequence of elementary flips.

Also, obtaining a periodic structure from an aperiodic initial region by a sequence of flips seems within this considered construction rather *difficult*.

5.1.2 Iterative Flip Approach – Eliminating Squares

Another way to investigate whether any Shield-Triangle tiling can be obtained by flips is to start with a local region of the Shield tiling and repeatedly flip the squares outward. The idea is that squares would gradually move away from the investigated region until only shields and triangles remain.

The example discussed in subsection 4.2 provides a suitable starting point for this investigation. After performing the flips shown there, all squares lie on the boundary of the flipped region, suggesting that they could be moved further outward by additional flips. In Figure 20 this oval-shaped region is embedded in a larger region of the tiling.

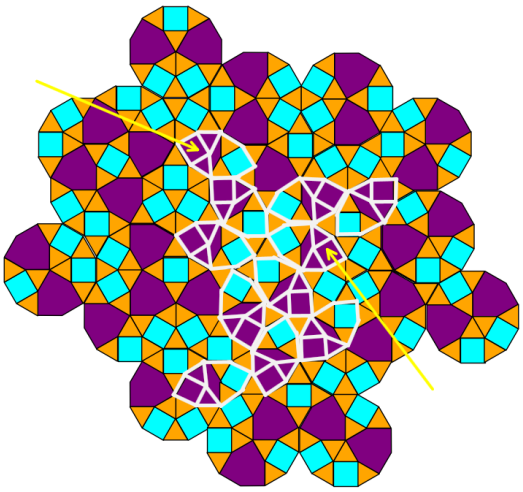

Figure 20: Larger region of the tiling with embedded flips. Inspecting the boundary of the performed flips (white) shows that the squares cannot be flipped further

The white shapes indicate additional flips that can be performed. In addition to the six flips already carried out, five more flips are possible. However, after these flips the process stops. Inspecting the boundary of the flipped region shows that no further flips can be performed.

Focusing on the white shape on the top left of the region, which is marked by a yellow arrow, reveals that if one wants to flip, there are no possibilities left to flip in this region. The same problem occurs on the right side. For the white square, which is also marked by a yellow arrow, no more allowed flips can be constructed. As a consequence, the shields accumulate in positions that prevent the formation of new flip possibilities. Indeed, this is the case for the entire boundary created by the white shapes. Therefore, one reaches a point at which no more flips are possible.

To resolve this issue, more complex moves have to be performed in order to propagate the squares further. For example, one could rotate several dodecagons adjacent to the white boundary. How dodecagons can be rotated is discussed in subsection 8.1. After such steps, squares can be transported further.

In conclusion, a tiling that consists of only dodecagons illustrated in Figure 14 seems within this examination not possible to achieve through flip sequences. The further idea to obtain any Shield Triangle tiling in a finite space is limited to the accumulation of tiles which do not have the required orientation in order to enable further flips. This

problem can be tackled by performing more complex flip sequences. This can also only be done in a limited range. This will be further discussed in subsubsection 5.3.1.

5.2 Square Triangle Tiling

The idea of eliminating certain tiles through flip sequences can also be applied to the Shield tile. One can try to obtain a tiling that consists only of squares and triangles.

For example, a possible dodecagon which consists only of squares and triangles is shown in Figure 21. Here, the tile and orientational based charge analysis yields the same result

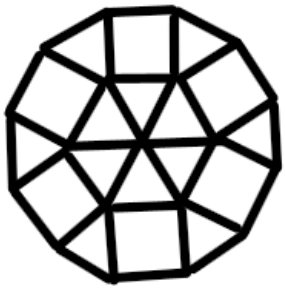

Figure 21: Dodecagon which only consists of squares and triangles [6]

as in subsection 5.1 since the tile charges compensate each other and no flip octagons can be identified in Figure 21. Hence, the same question arises: Is it possible to derive a tiling that is only made of squares and triangles?

5.2.1 Zipper moves

A natural idea is to use zipper moves to transport shields through the tiling. Such line like sequences of flips have been studied for the Square Triangle tiling in [17]. The basic idea is that a tile can be propagated along a line by performing a sequence of flips. If such zipper lines could be extended throughout the tiling, they might allow the shields to be pushed towards a boundary of a region and eventually be removed.

In the following example shown that zipper moves cannot transport shields arbitrarily far in the Square triangle tiling. In the Square Triangle tiling several types of zipper lines are possible. In Figure 22 two possible zipper lines are shown. The lines are generated by alternating flip octagons and allow a tile to move step by step along a line.

To test whether zipper moves can remove shields from a region, one can start by choosing a local symmetry center and attempt to move the shields towards a boundary using the zipper lines. The corresponding flip sequences are illustrated in Figure 23.

The flip sequence shown in Figure 23 illustrates how a shield can be propagated along a zipper line. In both cases the shield can indeed be moved several steps towards the

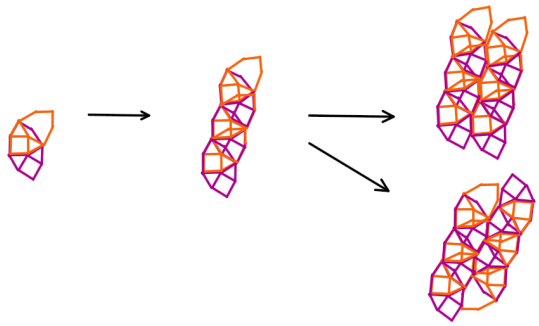

(a) Zipper lines formed by F_1 and F_3.
Top right: uniform orientation of lines
Bottom right: alternating orientation

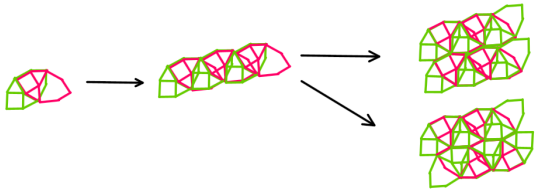

(b) Zipper lines formed by F_3 and F_5
Top right: uniform orientation of lines
Bottom right: alternating orientation

Figure 22: Two possible zipper lines following the idea of line tilings proposed in [16]

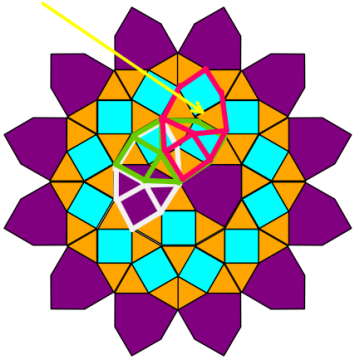

(a) Sequence of flips for moving the left middle shield towards the upper boundary of the region

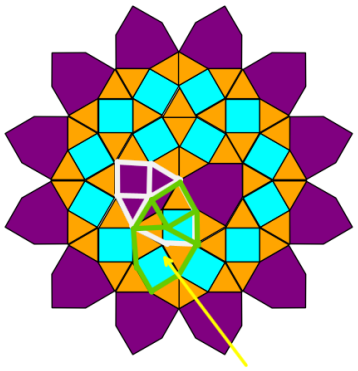

(b) Sequence of flips for moving the middle left shield towards the lower boundary of the region

Figure 23: Local symmetry center with marked shields (yellow arrow). The colored shapes indicate zipper lines starting with white followed by green and pink. The region confines the shields.

boundary of the region. However, this process stops after a finite number of flips. At the boundary of the region the required arrangement of the tiles for forming another flip octagon does not occur. As a consequence, the zipper line cannot continue.

Thus, zipper moves allow in finite regions with a fixed boundary to propagate shields, but arbitrarily far transport is not possible. Instead, the propagation terminates at the latest at the boundary of the region. Consequently, zipper moves alone cannot be used to remove the shields from the tiling in a finite region.

5.2.2 Iterative Flip Approach – Eliminating Shields

As an alternative approach, one can investigate again whether shields can be removed by performing local flips repeatedly. The idea is to start from a region that already resembles a Square Triangle tiling and to push the remaining shields further outwards. The region investigated in subsection 4.2 also provides a suitable starting point for this, as it already contains a relatively large area without shields. Starting from this region, flips are performed step by step in order to explore how far the shields can be propagated and where a simple sequence of flips eventually cannot be pursued further.

In contrast to the situation discussed in subsubsection 5.1.2, flips can be built constructively after the first sequence of flips. This is shown in Figure 24 where the successive flip sequences are marked in different colors.

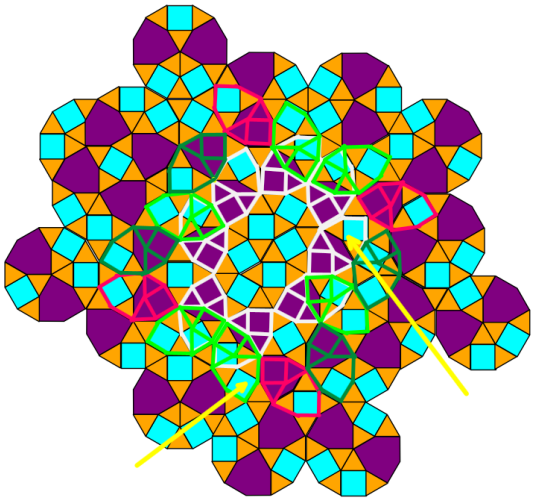

Figure 24: Iterations of performing a flip. The first sequence is indicated by white flips followed by constructively build light green flips. Pink and dark green ones are again simply constructable. Yellow arrows mark two examples in which the shields cannot be simply flipped. For further propagation more complex flips need to be performed in advance

However, this process does not continue indefinitely. After a finite number of steps, the simple propagation of the shield stops in some regions. The upper right arrow in Figure 24 marks such a termination of the sequence. The alignment of the edges of the surrounding tiles does not allow the formation of the required flip octagon for further flips. Similar situations occur at some other positions along the boundary. The propagation of shields stops after a finite number of simple steps, and the remaining shields cannot be moved any further away.

In order to propagate the shields further outward, one first has to perform a more complex sequence of flips. For example, one could rotate the dodecagon next to the left

arrow in Figure 24 (how this can be done is discussed in subsection 8.1). After a suitable rotation, more flips are possible, and the shield can be moved again.

5.3 Alternative ways to derive tilings

5.3.1 Inflation

After the discussion of performing flip sequences in finite region which fail at some point in generating a desired tiling, one can ask if there is another way to obtain this result. In addition to rearrangements such as flips, the tiling also allows a hierarchical transformation given by the inflation rules shown in Figure 25. Since inflation can also be applied repeatedly, it is natural to study how the charge behaves under one inflation step. In particular, one can investigate whether the charge remains invariant when the tiling is transformed to the next inflation level.

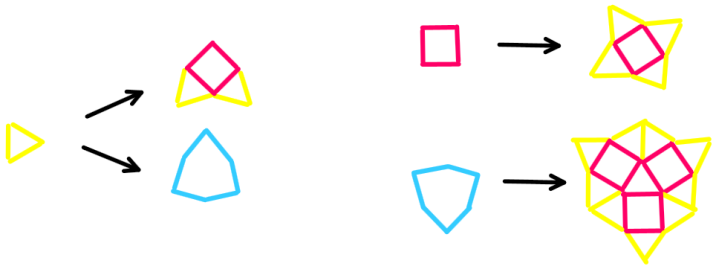

Figure 25: Inflation rules for the Shield tiling [6]

The inflation rules can be applied to a local symmetry center of the tiling. The resulting arrangement after one inflation step is shown in Figure 26.

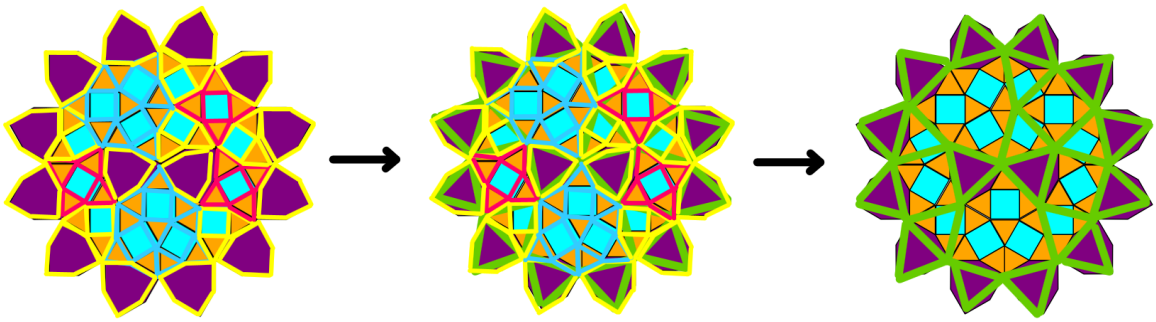

Figure 26: Local symmetry center of the tiling in which the inflation rules are applied which reveals how the region looks like after one inflation step

The green inflated region in Figure 26 is relative to the central dodecagon twisted by 65° as shown in Figure 27.

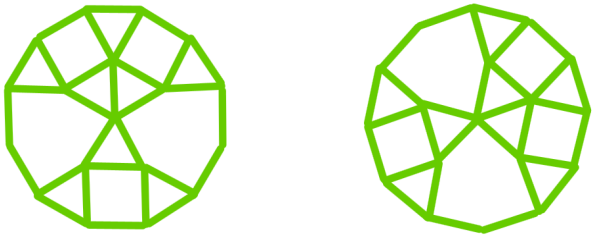

Figure 27: Inflated region which results in a dodecagon (right) is 65° rotated clockwise relative to the central dodecagon of the original region (left)

Since the charge measure is intended to quantify the symmetry of a region, it must not depend on the orientation of the coordinate system. A global rotation of all tiles corresponds to multiplying all phases by the same constant factor, but this does not change the relative arrangement of the tiles. Therefore, the inflated region can be rotated counterclockwise by 65° before evaluating the charge.

If one calculates the tile-charge in Figure 26 before the inflation step, which means all blue, yellow, and red tiles, and after the inflation step meaning, the green tiles, one finds

$$q_{\text{tot,infl}} - q_{\text{tot,ref}} = 7 - 7 = 0$$

Thus, apart from the constant global rotation introduced by the inflation step, the charge of the region remains unchanged and is therefore conserved.

One can calculate the flip charge by rotating the inflated dodecagon counterclockwise and identifying F_7 and F_8 then identifying the same flip octagons in the center of the initial region and subtracting them from each other, which yields

$$q_{\text{flip,infl}} - q_{\text{flip,ref}} = \left(11 - 2\sqrt{3}\right) - \left(59 + 2\sqrt{3}\right) = -48 - 4\sqrt{3}$$

One can now also apply the inflation step on larger regions evaluated for example, in subsection 4.3 which contain Figure 26 in the center.

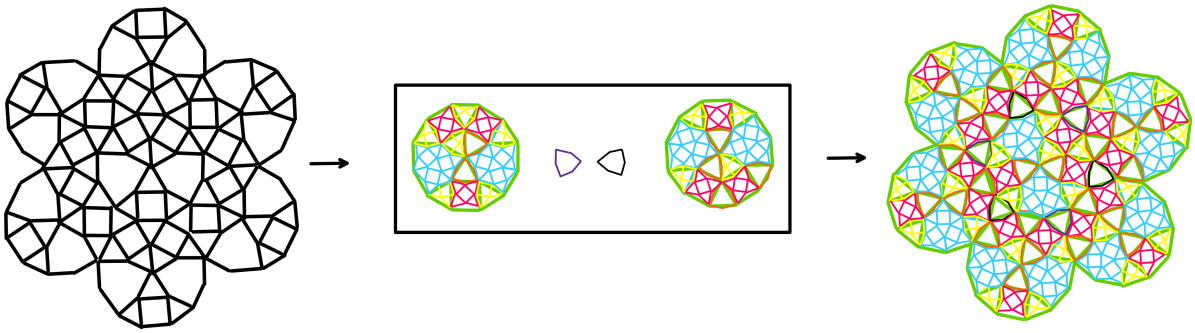

Figure 28: Inflation (left) and original region (right)

Calculating the tile charge in the inflated region (right in Figure 28) yields

$$q_{\text{tot,infl}} - q_{\text{tot,ref}} = 49 - 73 = -24.$$

Calculating the flip charge difference between the reference region and the inflated region yields

$$q_{\text{flip,infl}} - q_{\text{flip,ref}} = (59 + 2\sqrt{3}) - (83 + 2\sqrt{3}) = -24.$$

The value of the tile-/ and flip-charges of Figure 28 can be traced back to the six connection shield, which are sketched in black and purple. In the inflated region, these structures correspond to triangles whose contributions cancel each other and therefore do not contribute to the charge. In the reference region they correspond to shields, which allow the identification of flip octagons located outside the large inflated dodecagons. The change of the charges under an inflation step is therefore proportional to the number of connection tiles between the reference and the inflated region. Importantly, the analysis of flip contributions can in principle be carried out on the smaller structure just as on the inflated structure. However, a flip on the small scale does not necessarily correspond to a flip on the large scale. This means that Γ evaluated in the smaller region may not capture all contributions in the inflation step.

In principle, the structure of flips under inflation allows for a systematic analysis of the resulting charges. However, performing this analysis by hand becomes increasingly intensive for larger regions or multiple inflation steps. A computational approach, therefore could efficiently track the contributions of all flip octagons and connecting tiles, allowing one to quantify Γ and the tile charge changes at larger inflation steps.
Despite this limitation, the examples demonstrate the main principle. The change of charge under an inflation step is governed by the connection tiles and the flip based description is applicable at different scales.

Inflation rules provide, as discussed, a useful way to generate large regions of a tiling. In the case of the Square Triangle tiling one may attempt to derive alternative inflation rules without the Shield prototile. In order to investigate possible alternative inflation rules, a local symmetry center of the tiling is considered. Starting from this region, the shields are flipped outward as far as possible. In this way a region is obtained in which the central area consists only of squares and triangles.

From this region a patch slightly larger than a dodecagon is selected. Such a region is natural to consider since some Square Triangle tilings can be decomposed into such dodecagons. The selected patch is then resized to match the size of the inflated tiles in Figure 27. This is shown in Figure 29 in violet.

By placing this enlarged patch onto the original tiling, one can compare the inflated and reference region. In principle, this comparison could allow the identification of new

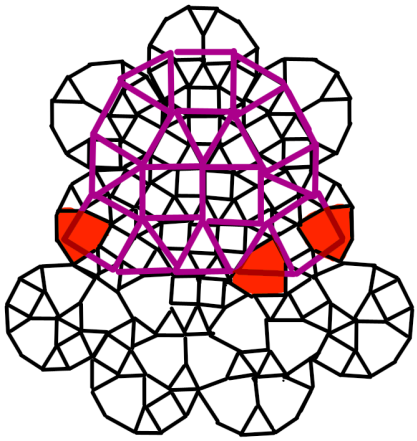

Figure 29: Schematic depiction of how alternate inflation rules can be derived. Inflated center of the region sketched in violet. Problematic tiles which prevent shield free alterative inflation rules are colored in red

inflation rules by determining which groups of proto tiles correspond to a single inflated tile.

However, in order for such a construction to work, the selected region would need to consist of squares and triangles. all shields would therefore have to be removed from the region beforehand. Although the flips push most of the shields towards the boundary, the region obtained after the maximal sequence of flips still contains shields near the boundary of the inflated region which are marked red in Figure 29. Since these shields cannot be removed by additional flips in the region, they obstruct the construction of alternate inflation rules. However, how this could be handled will be discussed in subsubsection 5.3.2.

In addition to shields appearing near the boundary, it is also not possible to derive a unique inflation rule from this example. Even in regions consisting only of squares and triangles, there are multiple possible ways to define how, for instance, the interior of a square should be inflated.
A similar approach could also be applied to the Shield Triangle tiling, where the existence of alternative inflation rules could be investigated in an analogous way.

5.3.2 Larger regions

A possible way besides rotating dodecagons to obtain suitable tile arrangements for flips is to try to enlarge the considered area. In principle, one could try to build the zipper lines introduced in subsubsection 5.2.1 and transport tiles in the region in which they are needed to form new flip octagons.

This could potentially solve the problem of tile accumulation in subsubsection 5.1.2, subsubsection 5.2.2 and subsubsection 5.3.1. In a theoretical framework, the tiling can

be assumed infinitely large and thus needed tiles could always be transported towards the region of interest. However, when dealing with finite regions, this procedure obviously cannot be applied. In this case, it is rather a question of how many flips are possible before no more options present themselves.

Whether it is always possible to construct zipper lines for transporting required tiles towards regions in which they are needed in order to perform flips or how many flips are possible inside a finite region is a question regarding combinatorics and can therefore be best investigated by computational methods through implementing the required theory. In this way, the question can maybe be answered, but this is beyond the scope of this work.

5.4 Other Possible Shield/Triangle/Square Tilings

Besides, the tilings discussed above, one may ask whether further tilings are possible.

First, note that a tiling consisting only of shields as defined in this work cannot exist. The interior angles of the shield tiles do not allow a consistent tessellation of the plane. [16]

Tilings consisting of only squares or triangles are geometrically possible in terms of interior angles. However, the examples discussed above suggest that such arrangements cannot be obtained by sequences of flips starting from the Shield tiling.

The examples discussed above indicate that sequences of flips are not sufficient to transform the Shield tiling into either a Shield Triangle or Square Triangle tiling. In all investigated constructions, the propagation of tiles eventually terminates because surrounding tiles do not allow the formation of new flip octagons. Consequently, the remaining tiles become confined in arrangements that prevent further transformations.

Of course, many further Shield Triangle and Square Triangle tiling exist beyond the specific examples considered here. Determining whether any of these are flip accessible from the Shield tiling would require a systematic exploration of large regions of the reference region. Such an investigation would require extensive computational methods and therefore lies beyond the scope of this work.

6 Penrose Tiling

The developed tools from section 2 can now also be applied to other tilings. For example, the generalized Penrose tiling [18] marks a suitable candidate. A section of said tiling is shown in Figure 30.

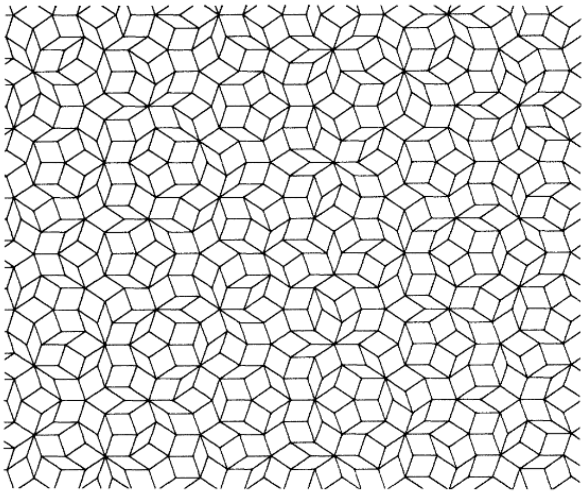

Figure 30: Generalized Penrose tiling in which flips are possible[18]

In this tiling, a possible flip has a similar occurrence compared to the one discussed above in the Shield tiling (Figure 3). The tiling and also the flip shown in Figure 31 is composed of flat (orange/dark blue) and acute rhombi (yellow/violet).

Figure 31: Possible flip in the generalized Penrose tiling. Arrows indicate how the orientation of the flip hexagon can be measured. Colors serves only illustrative purposes [19]

To evaluate the charges of the flip hexagons one first has to evaluate the complex phase of the involved charges. Since both prototiles exhibit the same rotational symmetry, one can calculate

$$z_{\mathrm{R}} = e^{2i\theta}. \tag{6.1}$$

In fact, in the Penrose tiling five different flips are possible. The flip partners are again hexagons, which lie opposite to each other in Figure 32. For example, F_1 and F_6 together form a flip pair.

The charge construction applied to the Penrose tiling listed in Table 7 yields a vanishing charge difference for all flip pairs. This indicates that the charge is conserved under flips

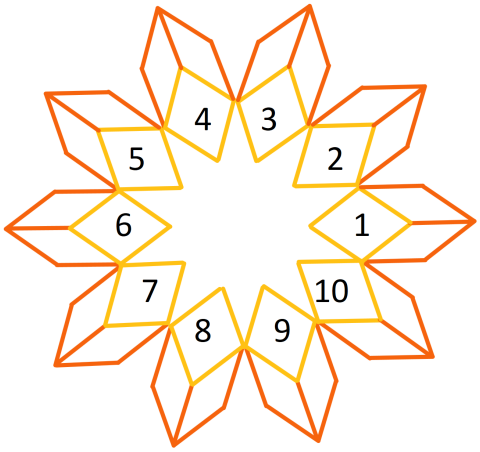

Figure 32: Different orientations of flip hexagons which can occur in the generalized Penrose tiling

Flip F_i	θ	Z_{tot}	q	Flip partner	q_{flip}	$\Delta q = q_{\text{flip}} - q$
F_1	$\frac{0\pi}{5}$	$\frac{5}{10} - \frac{15}{10}i$	$\frac{5}{2}$	F_6	$\frac{5}{2}$	0
F_2	$\frac{1\pi}{5}$	$-\frac{13}{10} + \frac{9}{10}i$	$\frac{5}{2}$	F_7	$\frac{5}{2}$	0
F_3	$\frac{2\pi}{5}$	$-\frac{13}{10} - \frac{9}{10}i$	$\frac{5}{2}$	F_8	$\frac{5}{2}$	0
F_4	$\frac{3\pi}{5}$	$\frac{5}{10} - \frac{15}{10}i$	$\frac{5}{2}$	F_9	$\frac{5}{2}$	0
F_5	$\frac{4\pi}{5}$	$\frac{16}{10}$	$\frac{64}{25}$	F_{10}	$\frac{64}{25}$	0
F_6	$\frac{5\pi}{5}$	$\frac{5}{10} - \frac{15}{10}i$	$\frac{5}{2}$	F_1	$\frac{5}{2}$	0
F_7	$\frac{6\pi}{5}$	$-\frac{13}{10} + \frac{9}{10}i$	$\frac{5}{2}$	F_2	$\frac{5}{2}$	0
F_8	$\frac{7\pi}{5}$	$-\frac{13}{10} - \frac{9}{10}i$	$\frac{5}{2}$	F_3	$\frac{5}{2}$	0
F_9	$\frac{8\pi}{5}$	$\frac{5}{10} - \frac{15}{10}i$	$\frac{5}{2}$	F_4	$\frac{5}{2}$	0
F_{10}	$\frac{9\pi}{5}$	$\frac{16}{10}$	$\frac{64}{25}$	F_5	$\frac{64}{25}$	0

Table 7: Orientation angle θ, Z_{tot} complex phase of all hexagon tiles together, charge of the hexagon q, flip partner, corresponding charge of the flip partner q_{flip} and charge differences Δq between the two charges. Colored rows indicate pairs of the same Z_{tot} value

in the tiling. In contrast, the Shield tiling exhibits several distinct charge differences, suggesting that flips there involve changes that affect the charge assignment. Consequently, the method introduced in section 2 does not provide additional information on the flip dynamics in the Penrose tiling. This suggests that the definition of a charge may mainly be useful for tilings in which transformations change the charge of the flip.

In the case of the Penrose tiling, a different approach may be more suitable to analyze structural changes. Instead of considering the change obtained from the square of the absolute value, one can study the total complex phase Z_{tot} which is calculated by

evaluating the complex contribution of each tile and summing all contributions. In this case four different values are obtained (colored rows in Table 7), while only two distinct charges appear when considering the charge q which is the square of the absolute value of Z_{tot}.

However, the complex phase generally depends on the choice of the coordinate system. The use of absolute square, removes this dependence and yields a rotational invariant quantity. When working directly with the complex phase, this coordinate dependence therefore has to be treated separately. How this dependence can be treated in a consistent way remains an open question and would require a more detailed analysis.

Another approach to obtain a more suitable expression for a characterization could be to take the interior angles of the tiles into account, in analogy to the shield tile in section 2. How this can be done also requires further research.

7 Conclusion

The examples provided in this work demonstrate that the tile based analysis together with the flip and orientational based analysis provide complementary insights into the tile rearrangements caused by flips.
However, the analysis also reveals certain limitations. Different sequences of flips may lead to identical values of the change while producing different final tilings. Therefore, a construction of a tiling based on a given charge difference is always possible, but not unique, in this framework.
A possible approach to resolve this issue can be to construct the charges of the flip octagons in such a way that every pair results in a different charge difference. In this work, the charge differences are solely based on the symmetry and orientation of the tiles. Whether it is possible to construct charge differences with unique values only based on geometrical considerations remains an open question.

Furthermore, attempts to construct specific tilings through flip sequences in finite regions within the Shield tiling are limited by the accumulation of tiles with unfortunate orientations. In particular, the generation of tilings consisting of only shields and triangles and tilings of squares and triangles appears to be not achievable within the considered framework.
These observations suggest that additional mechanisms may be required to systematically construct the desired tilings. Possible approaches include investigating alternative inflation rules or considering larger regions in which tiles can be transported through zipper lines.

The analysis of the Penrose tiling shows that the charge construction does not always provide additional information about the flip process. For all pairs of flips, the charge difference vanishes, indicating that the charge is conserved under flip operations, suggesting that the definition of a charge may mainly be useful for tilings in which flips change the charge of the flip. How charges can be constructed meaningfully in such tilings remains an open question for future work.

Overall, the presented framework provides a systematic way to analyze flip induced rearrangements in aperiodic tilings and suggests several directions for further investigation. Interesting questions include a systematic classification of the flip sequences and closely related to that the flip accessibility of different tilings, paired with computational approaches to further investigate flip dynamics.

8 Appendix

8.1 Flips in Dodecagons and how to derive them

As discussed above, the Shield tiling contains smaller dodecagonal structures. Within these structures flips can also be performed. It the flips are restricted to this region the dodecagon can be rotated in discrete steps of 30°. This is useful when analyzing larger structures that are composed of such dodecagons since the orientation of these regions can first be adjusted in order to create a flip sequence. Afterwards if required one can identify which flips within the dodecagon were responsible for the rotation.
The dodecagons shown in Figure 33 illustrate how flips within the dodecagon generate different orientations of the same structure in the second and third row. Starting from four positions of the square which lays opposite to the other two, a sequence of flips lead to all twelve possible orientations. The figure also shows additional possibilities of arrangements in which the the three squares are located on the same side of the dodecagon.

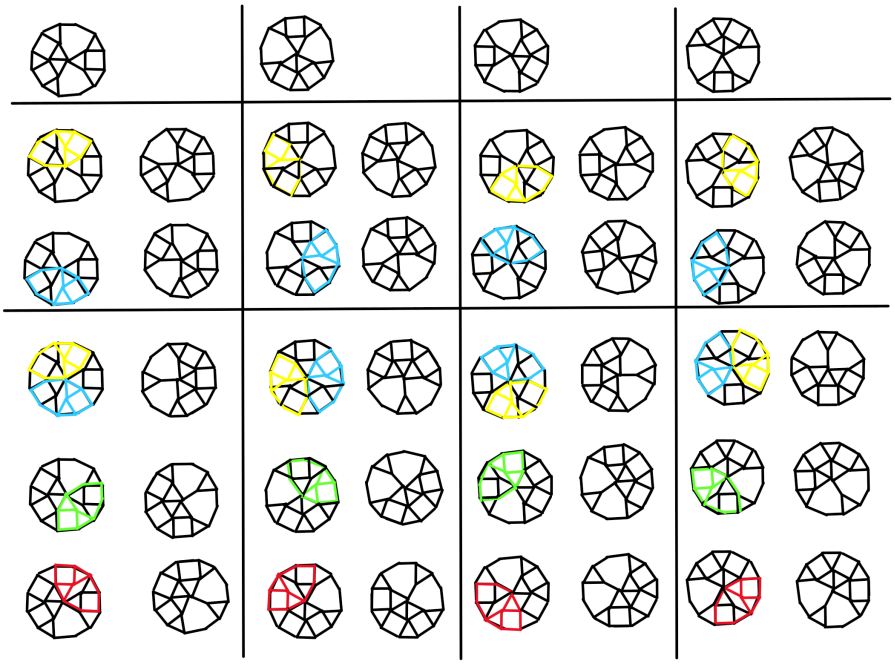

Figure 33: Flips in dodecagons at starting positions $1, -i, -1$ and i measured with respect to the square opposite to the other two. These starting configurations generate all twelve possible orientations of the dodecagon shown in the second and third rows. In addition flips are possible in which all three squares lie on one side of the dodecagon. These are shown in row three, four and five.

The transition between the four basic starting positions are summarized in Figure 34 which show the flip sequences required to move between them.

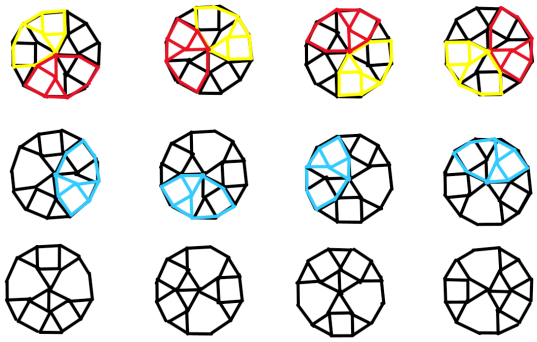

Figure 34: Flips required to switch between the four starting positions shown in the first row in Figure 33

8.2 Ambiguity of Identification

In the examples discussed previously the flip octagons were preferred identified whose squares shared a common vertex. However the general difficulty in these reference regions arises from the ambiguity of how the flip octagons can be identified. For example in Figure 35 four distinct flip octagons namely F_3, F_6, F_{10} and F_{11} can be identified. The figure also illustrates several possible ways in which two flip octagons can be selected from these candidates.

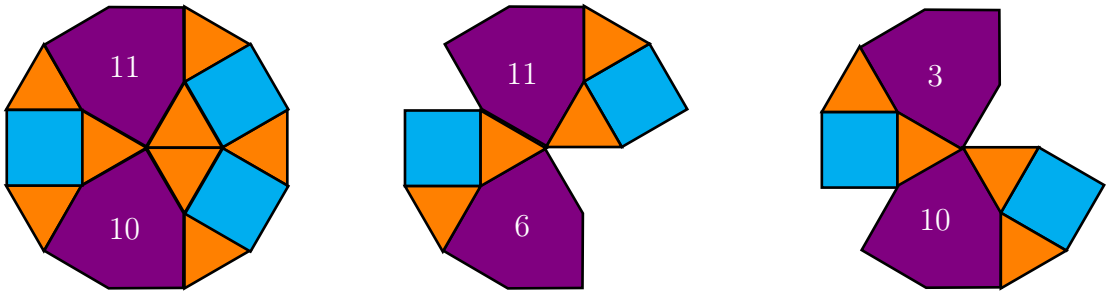

Figure 35: Dodecagon with all possibilities to identify two unique flip octagons

If one chooses a square opposite to the other two as a reference point and rotates the dodecagon in steps of 30° one can determine which flip octagons can be uniquely identified in each dodecagon. For every orientation the goal is to identify the maximal number of uniquely determined flip octagons which in this case is two. The corresponding flip charges are then added. The resulting values are listed in Table 8. The region shown in Figure 35 corresponds to the orientation in which the reference square is rotated by 180°.

Angle	Shared vertex	Square 1	Square 2
120°	(12,1) 7- $2\sqrt{3}$	(1,8) 7+ $2\sqrt{3}$	(12,5) 10-42$\sqrt{3}$
90°	(1,2) 5	(2,9) 8 + $2\sqrt{3}$	(1,6) 5
60°	(2,3) 6	(3,10) 9	(2,7) 9
30°	(3,4) 5	(4,11) 5	(3,8) 8+$2\sqrt{3}$
0°	(4,5) 7- $2\sqrt{3}$	(5,12) 10 - $42\sqrt{3}$	(4,9) 7 + $2\sqrt{3}$
330°	(5,6) 8- $2\sqrt{3}$	(6,1) 5	(5,10) 11- $2\sqrt{3}$
300°	(6,7) 9	(7,2) 9	(6,11) 6
270°	(7,8) 11 + $2\sqrt{3}$	(8,3) 8 + $2\sqrt{3}$	(7,12) 11- $2\sqrt{3}$
240°	(8,9) 10 + $2\sqrt{3}$	(9,4) 7 + $2\sqrt{3}$	(8,1) 7 +$2\sqrt{3}$
210°	(9,10) 11 + $2\sqrt{3}$	(10,5) 11- $2\sqrt{3}$	(9,2) 8+ $2\sqrt{3}$
180°	(10,11) 9	(11,6) 6	(10,3) 9
150°	(11,12) 8 - $2\sqrt{3}$	(12,7) 11- $2\sqrt{3}$	(11,4) 5

Table 8: Possible flip charges inside a dodecagon. Based on the position of the square opposing the other two the dodecagon can be shifted in 30° steps. Inside the dodecagon three different possibilities for the identification of flip octagons arise. One in which the squares share a vertex and two in which this is not the case. Colors illustrate rows with the same charge values

9 References

[1] Luwei Zhou. *Introduction to Soft Matter Physics*. World Scientific, 2019.

[2] D. Shechtman, I. Blech, D. Gratias, and J. W. Cahn. Metallic phase with long-range orientational order and no translational symmetry. *Phys. Rev. Lett.*, 53:1951–1953, Nov 1984.

[3] Dov Levine and Paul Joseph Steinhardt. Quasicrystals: A new class of ordered structures. *Phys. Rev. Lett.*, 53:2477–2480, Dec 1984.

[4] Marjorie Senechal. *Quasicrystals and geometry*. Cambridge University Press, 1995.

[5] E. Harriss D. Frettlöh, F. Gähler. Tilings encyclopedia, 2026. https://tilings.math.uni-bielefeld.de/ [last access on 14.04.2026].

[6] Michael Baake and Uwe Grimm. *Aperiodic Order. Volume 1: A Mathematival Invitation*. Cambridge University Press, 2015.

[7] P.M. Chaikin and T.C. Lubensky. *Priniciples of condensed matter physics*. Cambridge University Press, 1995.

[8] Marko V. Jaric. *Aperiodicity and Order Volume 2 – Introduction to the Mathematics of Quasicrystals*. Academic Press, 1989.

[9] Franz Gähler. Crystallography of dodecagonal quasicrystals. *pp. 272-284 in Quasicrystalline Materials*, World Scientific 1988. http://dx.doi.org/10.18419/opus-7047.

[10] B. I. Halperin and David R. Nelson. Theory of two-dimensional melting. *Phys. Rev. Lett.*, 41:121–124, Jul 1978.

[11] David R. Nelson. *Defects and Geometry in Condensed Metter Physics*. Cambridge University Press, 2002.

[12] Paul J. Steinhardt, David R. Nelson, and Marco Ronchetti. Bond-orientational order in liquids and glasses. *Phys. Rev. B*, 28:784–805, Jul 1983.

[13] Michael Engel and Hans-Rainer Trebin. Self-assembly of monatomic complex crystals and quasicrystals with a double-well interaction potential. *Phys. Rev. Lett.*, 98:225505, Jun 2007.

[14] Marianne Imperor-Clerc, Pavel Kalugin, Sebastian Schenk, Wolf Widdra, and Stefan Förster. Higher-dimensional geometrical approach for the characterization of two-dimensional square-triangle-rhombus tilings. *Phys. Rev. B*, 110:144106, Oct 2024.

[15] Olivier Bodini, Thomas Fernique, and Éric Rémila. A characterization of flip-accessibility for rhombus tilings of the whole plane. *Information and Computation*, 206(9):1065–1073, 2008. https://doi.org/10.1016/j.ic.2008.03.008.

[16] Thomas Fernique and Olga Mikhailovna Sizova. Shield tilings, 2023. https://doi.org/10.48550/arXiv.2305.17737.

[17] Mark Oxborrow and Christopher L. Henley. Random square-triangle tilings: A model for twelvefold-symmetric quasicrystals. *Phys. Rev. B*, 48:6966–6998, Sep 1993. https://link.aps.org/doi/10.1103/PhysRevB.48.6966.

[18] Michel Duneau and André Katz. Quasiperiodic patterns. *Phys. Rev. Lett.*, 54:2688–2691, Jun 1985.

[19] Attila Szállás and Anuradha Jagannathan. Phason disorder effects in the penrose tiling antiferromagnet. *Zeitschrift für Kristallographie - Crystalline Materials*, 224, 11 2008.

Muster für eine Eigenständigkeitserklärung

Hiermit versichere ich, Anna Milard (Name) 23115524 (Matrikelnummer), die vorgelegte Arbeit selbstständig und ohne unzulässige Hilfe Dritter sowie ohne die Hinzuziehung nicht offengelegter und insbesondere nicht zugelassener Hilfsmittel angefertigt zu haben. Die Arbeit hat in gleicher oder ähnlicher Form noch keiner anderen Prüfungsbehörde vorgelegen und wurde auch von keiner anderen Prüfungsbehörde bereits als Teil einer Prüfung angenommen.

Die Stellen der Arbeit, die anderen Quellen im Wortlaut oder dem Sinn nach entnommen wurden, sind durch Angaben der Herkunft kenntlich gemacht. Dies gilt auch für Zeichnungen, Skizzen, bildliche Darstellungen sowie für Quellen aus dem Internet.

Mir ist insbesondere bewusst, dass die Nutzung künstlicher Intelligenz verboten ist, sofern diese nicht ausdrücklich als Hilfsmittel von dem Prüfungsleiter bzw. der Prüfungsleiterin zugelassen wurde. Dies gilt insbesondere für Chatbots (insbesondere ChatGPT) bzw. allgemein solche Programme, die anstelle meiner Person die Aufgabenstellung der Prüfung bzw. Teile derselben bearbeiten könnten.

Verstöße gegen die o.g. Regeln sind als Täuschung bzw. Täuschungsversuch zu qualifizieren und führen zu einer Bewertung der Prüfung mit „nicht bestanden".

Erlangen, 14.04.2026
Ort, Datum

Eigenhändige Unterschrift